RESEARCH ARTICLE SUMMARY

PLANT SCIENCE

A Gγ protein regulates alkaline sensitivity in crops

Huili Zhang†, Feifei Yu†*, Peng Xie†, Shengyuan Sun†, Xinhua Qiao†, Sanyuan Tang, Chengxuan Chen, Sen Yang, Cuo Mei, Dekai Yang, Yaorong Wu, Ran Xia, Xu Li, Jun Lu, Yuxi Liu, Xiaowei Xie, Dongmei Ma, Xing Xu, Zhengwei Liang, Zhonghui Feng, Xiahe Huang, Hong Yu, Guifu Liu, Yingchun Wang, Jiayang Li, Qifa Zhang, Chang Chen, Yidan Ouyang*, Qi Xie*

INTRODUCTION: According to the Food and Agriculture Organization (FAO), there are currently >1 billion ha of land affected by salt. Among these, ~60% are classified as sodic soil areas. These have high pH and are dominated by sodium bicarbonate ($NaHCO_3$) and sodium carbonate (Na_2CO_3). The effects of global warming and a lack of fresh water will lead to >50% of arable land becoming affected by salt by 2050, thus severely affecting the world's food security. Identifying and/or engineering sodic-tolerant crops is imperative to solve this challenge. Although salinity tolerance has been studied extensively, alkalinity tolerance in plants has not been studied in depth.

RATIONALE: Sorghum originates from Africa, where it can grow in harsh environments. As a result, sorghum has evolved greater tolerance to adapt to multiple abiotic stresses compared with other crops. Some sorghum varieties can survive in sodic soil with a pH as high as 10.0. A genome-wide association study (GWAS) analysis was performed with a large sorghum association panel consisting of 352 representative sorghum accessions. We detected a major locus, *Alkaline tolerance 1* (*AT1*), linked to alkaline tolerance. We found that *AT1*, encoding an atypical G protein γ subunit (a homolog to rice *GS3*), contributes to alkaline sensitivity by modulating the efflux of hydrogen peroxide (H_2O_2) under environmental stress.

RESULTS: On the basis of the results of the GWAS analysis, we sequenced the cDNA regions of *SbAT1* (*Sorghum bicolor AT1*) in 37 sorghum accessions with different degrees of alkaline sensitivity. Two typical haplotypes (Hap1 and Hap2) of *SbAT1* were identified according to the five leading variant sites associated with sorghum alkali sensitivity. Hap1 encodes an intact SbAT1. A frame shift mutation (from "G" to "GGTGGC") within Hap2 results in a premature stop codon probably encoding a truncated protein with only 136 amino acids at the N terminus (named *Sbat1*).

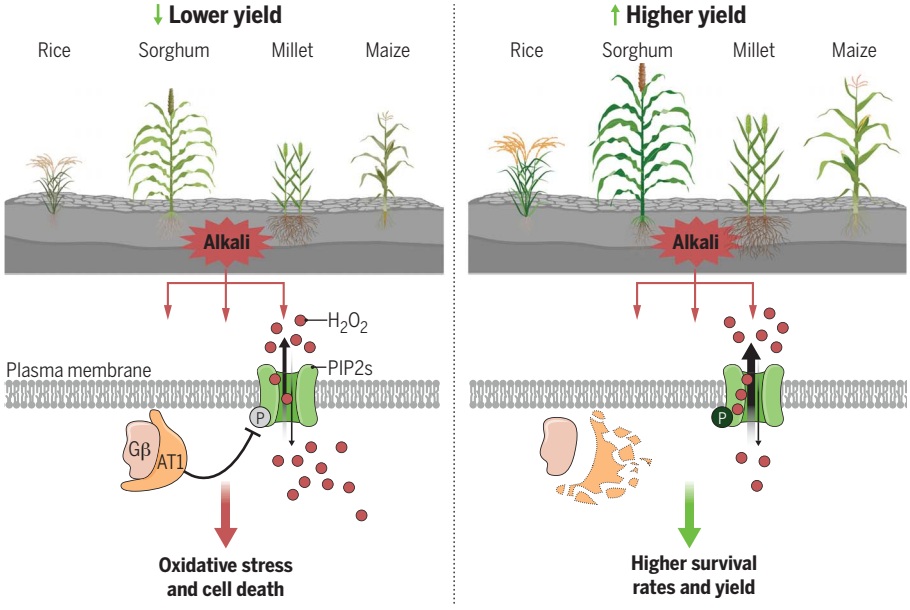

Genetic modification of AT1 enhances alkaline stress tolerance. The Gγ subunit, AT1, pairs with Gβ to negatively modulate the phosphorylation level of PIP2 aquaporins. Thus, AT1 reduces the H_2O_2 export activity of PIP2s, leading to the overaccumulation of H_2O_2 and resulting in alkaline stress sensitivity. By contrast, the artificial or natural knockouts of *AT1* homologs release the inhibition of PIP2s by AT1 in crops and have improved survival rates and yield under alkaline stress. [Figure created using BioRender]

To confirm the function of the *AT1* locus, we generated a pair of near-isogenic lines (NILs) with two *AT1* haplotypes to assess the allelic effect of *AT1* on sorghum tolerance to alkali. We found that the *Sbat1* allele (Hap2), encoding a truncated form of SbAT1, increased plant alkaline sensitivity compared with wild-type full-length *SbAT1* (Hap1). Overexpression of *AT1/GS3* reduced alkaline tolerance in sorghum and rice, and overexpression of the C-terminal truncated AT1/GS3 showed a more severe alkaline sensitive response. This was confirmed in millet and rice, which suggests that *AT1/GS3* functions negatively in plant alkali tolerance. By contrast, knockout (ko) of *AT1/GS3* increased tolerance to alkaline stress in sorghum, millet, rice, and maize, which indicates a conserved pathway in monocot crops.

By immunoprecipitation in combination with mass spectrometry (IP-MS), we found that AT1/GS3 interacts with aquaporin PIP2s that are involved in reactive oxygen species (ROS) homeostasis. Genetic analysis showed that $OsPIP2;1^{ko}/2;2^{ko}$ had lower alkaline tolerance than their wild-type control. The redox probe Cyto-roGFP2-Orp1 sensing H_2O_2 in the cytoplasm was applied. The results showed that, upon alkaline treatment, the relative H_2O_2 level increased in $OsPIP2;1^{ko}/2;2^{ko}$ compared with wild-type plants. These results suggested that the phosphorylation of aquaporins could modulate the efflux of H_2O_2. Gγ negatively regulates the phosphorylation of PIP2;1, leading to elevated ROS levels in plants under alkaline stress. To assess the application of the *AT1/GS3* gene for crop production, field tests were carried out. We found that the nonfunctional mutant, either obtained from natural varieties or generated by gene editing in several monocots, including sorghum, millet, rice, and maize, can improve the field performance of crops in terms of biomass or grain production when cultivated on sodic lands.

CONCLUSION: We concluded that *SbAT1* encodes an atypical G protein γ subunit and inhibits the phosphorylation of aquaporins that may be used as H_2O_2 exporters under alkaline stress. With this knowledge, genetically engineered crops with knockouts of *AT1* homologs or use of natural nonfunctional alleles could greatly improve crop yield in sodic lands. This may contribute to maximizing the use of global sodic lands to ensure food security. ■

The list of author affiliations is available in the full article online.
*Corresponding author. Email: qxie@genetics.ac.cn (Q.X.); ffyu@cau.edu.cn (F.Y.); diana1983941@mail.hzau.edu.cn (Y.O.)
†These authors contributed equally to this work.
Cite this article as H. Zhang *et al.*, *Science* **379**, eade8416 (2023). DOI: 10.1126/science.ade8416

READ THE FULL ARTICLE AT
https://doi.org/10.1126/science.ade8416

RESEARCH ARTICLE

PLANT SCIENCE

A Gγ protein regulates alkaline sensitivity in crops

Huili Zhang[1,2]†, Feifei Yu[1,3]†*, Peng Xie[1]†, Shengyuan Sun[4,5]†, Xinhua Qiao[6]†, Sanyuan Tang[1], Chengxuan Chen[1], Sen Yang[1,7], Cuo Mei[1,7], Dekai Yang[1,7], Yaorong Wu[1], Ran Xia[1], Xu Li[4], Jun Lu[4], Yuxi Liu[4], Xiaowei Xie[2], Dongmei Ma[2], Xing Xu[2], Zhengwei Liang[8], Zhonghui Feng[7,8], Xiahe Huang[1], Hong Yu[1], Guifu Liu[1], Yingchun Wang[1,7], Jiayang Li[1,7], Qifa Zhang[4], Chang Chen[6,7], Yidan Ouyang[4]*, Qi Xie[1,7,9]*

The use of alkaline salt lands for crop production is hindered by a scarcity of knowledge and breeding efforts for plant alkaline tolerance. Through genome association analysis of sorghum, a naturally high-alkaline–tolerant crop, we detected a major locus, *Alkaline Tolerance 1* (*AT1*), specifically related to alkaline-salinity sensitivity. An *at1* allele with a carboxyl-terminal truncation increased sensitivity, whereas knockout of *AT1* increased tolerance to alkalinity in sorghum, millet, rice, and maize. *AT1* encodes an atypical G protein γ subunit that affects the phosphorylation of aquaporins to modulate the distribution of hydrogen peroxide (H_2O_2). These processes appear to protect plants against oxidative stress by alkali. Designing knockouts of *AT1* homologs or selecting its natural nonfunctional alleles could improve crop productivity in sodic lands.

Food security is affected by the growth of human populations worldwide and the potential negative impacts of climate change on agricultural production. Weather patterns resulting from global warming may limit fresh water availability. In the near future, saline soils are estimated to increase in ~50% of irrigated lands as a result of the application of chemical fertilizers (*1*). Consequently, soil salinity may become a global problem affecting plant growth and crop production. Use of these saline lands for crop production could help meet future food demands. Therefore, breeding more salinity-tolerant crops will likely be prioritized in the future of agriculture.

[1]State Key Laboratory of Plant Genomics, Institute of Genetics and Developmental Biology, The Innovative Academy of Seed Design, Chinese Academy of Sciences, Beijing 100101, China. [2]Breeding Base of State Key Laboratory of Land Degradation and Ecological Restoration of North Western China, School of Agriculture, Ningxia University, Yinchuan 750021, China. [3]College of Grassland Science and Technology, China Agricultural University, Beijing 100083, China. [4]National Key Laboratory of Crop Genetic Improvement and National Centre of Plant Gene Research (Wuhan), Hubei Hongshan Laboratory, Huazhong Agricultural University, Wuhan 430070, China. [5]Jiangsu Key Laboratory of Crop Genetics and Physiology and Co-Innovation Center for Modern Production Technology of Grain Crops, Key Laboratory of Plant Functional Genomics of the Ministry of Education, Yangzhou University, Yangzhou 225009, China. [6]National Laboratory of Biomacromolecules, CAS Center for Excellence in Biomacromolecules, Institute of Biophysics, Chinese Academy of Sciences, Beijing 100101, China. [7]University of Chinese Academy of Sciences, Beijing 100049, China. [8]Northeast Institute of Geography and Agroecology, Daan National Station for Agro-ecosystem Observation and Research, Chinese Academy of Sciences, Changchun 130102, China. [9]National Center of Technology Innovation for Maize, State Key Laboratory of Maize Germplasm Innovation and Molecular Breeding, Syngenta Group China, Beijing 102206, China.
***Corresponding author. Email: qxie@genetics.ac.cn (Q.X.); ffyu@cau.edu.cn (F.Y.); diana1983941@mail.hzau.edu.cn (Y.O.)**
†These authors contributed equally to this work.

On the basis of research by the Food and Agriculture Organization (FAO) of the United Nations (in 2015; https://www.fao.org/3/i5199e/i5199e.pdf), there are >1 billion ha of land affected by salt, and ~60% of the estimated area was classified as sodic [land with a high pH because of high alkali contents dominated by sodium bicarbonate ($NaHCO_3$) and sodium carbonate (Na_2CO_3)]. About 25 to 33% of the irrigated land worldwide is affected by secondary salinity (*2*). In analyzing publications from the past 20 years on Web of Science (https://www.webofscience.com/), we discovered that the number of published studies relevant to salt tolerance was up to 22,614 compared with only 457 for alkalinity tolerance. Because of insufficient knowledge about alkaline stress, technological development to increase crop production in saline-alkali soil has been limited. Different from neutral salinity (pH of ~7) with only ion toxicity, high pH in alkaline saline soil reduces the uptake rates of essential nutrients and sodium ion (Na^+) exclusion. This leads to more negative consequences on plant growth by inducing high cellular oxidative stress compared with salinity alone (*3*). Sorghum is currently the fifth main food crop in the world. It originates from Africa's harsh environments and has evolved a greater ability to adapt to some abiotic stresses compared with other crops. Thus, it is considered a useful resource for the discovery of mechanisms and genetic resources to improve crop responses to environmental stress, including alkaline stress (*4*).

High alkalinity boosts hydrogen peroxide (H_2O_2) levels in cells and causes oxidative damage to cellular proteins, lipids, and DNA, which results in apoptosis (*5*–*7*). Aquaporins (AQPs) are conserved from prokaryotes to eukaryotes. They are tetrameric, membrane-bound channels known to facilitate bidirectional transport of water and other small solutes across cell membranes. Researchers have reported that several members of the aquaporin superfamily in various organisms can also transport the redox signaling compound, H_2O_2, to facilitate the fine adjustment of H_2O_2 levels in the cytoplasm (*8*). Tong *et al.* (*9*) found that aquaporins from *Streptococcus* acted as peroxiporins for the efflux of intracellular H_2O_2 to alleviate oxidative stress. A study on the mammalian lens aquaporin, AQP5, showed that under hyperglycemic stress conditions with a higher level of intracellular H_2O_2, AQP5 facilitated H_2O_2 efflux from cells to maintain balance and homeostasis of H_2O_2 levels (*10*). In plants, aquaporins are involved in different stress defenses, and their phosphorylation plays an essential role in their transport activity (*11*, *12*). However, how crops sense alkaline stress and how the subsequent signaling affects H_2O_2 transport has yet to be explored.

Membrane-bound G proteins are conserved across the eukaryotic kingdom. They are heterotrimeric proteins bound to guanine nucleotides and consist of three subunits—G protein alpha (Gα), beta (Gβ), and gamma (Gγ). They play diverse roles in development and environmental interactions throughout an organism's life cycle. There are large numbers of diverse G protein γ subunits in plants with functions in different aspects of signal perception, transduction, and regulation of downstream effectors (*13*). Although G protein signaling pathways are well studied in mammals, the underlying mechanisms associated with G protein γ subunits in plants, especially in abiotic stress signaling, remain unclear.

In this work, we discovered *Alkaline Tolerance 1* (*AT1*, which encodes an atypical G protein γ subunit) showing alkaline tolerance in sorghum by genome-wide association study (GWAS) analysis. We reveal a conserved mechanism in which the G protein γ subunit modulates the phosphorylation of aquaporins to regulate reactive oxygen species (ROS) levels to maintain H_2O_2 homeostasis. This forms part of the plant protective response against oxidative stress caused by alkaline conditions. On the basis of this knowledge, we genetically edited the homologous gene of *AT1* in other crops to increase rice, maize, and millet alkaline tolerance in saline-alkali soils.

The AT1 locus is linked to alkaline tolerance

Sorghum has a specific tolerance to sodic soil, and some varieties can survive in a pH as high as 10.0 (*14*, *15*). To mimic the various saline-alkali conditions that may be found in saline-sodic soils in the field, we first tested different concentrations of mixtures of two alkali salts ($NaHCO_3$ and Na_2CO_3) and measured their effects on the survival rates of sorghum seedlings.

A mixture of alkali salts was used because it should produce a relatively stable pH range throughout various treatment periods. Different time periods of treatments were used on 16 selected sorghum accessions based on seed availability (table S1). Analysis of relative survival rates (a ratio of the survival rate under stress treatment to that without stress treatment) showed that after 21 days of treatment, the concentration of 75 mM mixed alkali salts (62.5 mM $NaHCO_3$ and 12.5 mM Na_2CO_3; pH = 9.2 to 9.4) showed the widest range in variation of rates and was the most reliable treatment to evaluate alkaline tolerance in sorghum (fig. S1, A to C). We then evaluated relative survival rates from a large sorghum association panel consisting of 352 representative sorghum accessions, and we observed that ~22% of the sorghum accessions exhibited high tolerance to alkali conditions with relative survival rates reaching >80%, whereas ~13% of sorghum accessions showed high sensitivity to alkalinity with relative survival rate no more than 20%. The frequency distribution in relative survival rate phenotypes of our sorghum population indicated that relative survival rate might be a useful index for genetic association analysis (fig. S1, D and E).

Using the above relative survival rate phenotypic data and a single-nucleotide polymorphism (SNP) genotype dataset for this panel, we performed a GWAS and identified two major loci ($P < 1.0 \times 10^{-5}$) linked with alkaline tolerance, both of which were located on the long arm of chromosome 1 (Fig. 1A and fig. S1F). We found a leading SNP (*S1_55779338*) located inside the annotated gene *Sobic.001G341700*, which was named *Alkaline Tolerance 1* (*SbAT1*) (Fig. 1B). *SbAT1* is predicted to encode an atypical G protein γ subunit of 198 amino acids in length, which includes a Gγ-like domain in the N terminus and a cysteine-rich domain in the C terminus. SbAT1 shares 55.56% protein sequence identity with OsGS3 in rice (*16*) and 82.30% protein sequence identity with ZmGS3 (*17*) in maize. To verify whether the sequence polymorphisms of *SbAT1* were correlated with alkaline tolerance in sorghum, we sequenced the cDNA region of *SbAT1* in 37 sorghum accessions with different degrees of alkaline stress tolerance. A total of 29 sequence variation sites were found, and five of them showed strong association signals ($P = 1.0 \times 10^{-3}$ to 1.0×10^{-5}) between the natural variations and relative survival rates in the 75 mM alkali treatment. Linkage disequilibrium (LD) analysis also indicated that the five leading association signals (positioned at +3863, +4151, +4157, +4438, and +4463) were attributable to high LD values [coefficient of determination (R^2) > 0.9] (Fig. 1C).

On the basis of sequence variations of the five leading sites, the selected 37 sorghum accessions from other stock (table S1) were

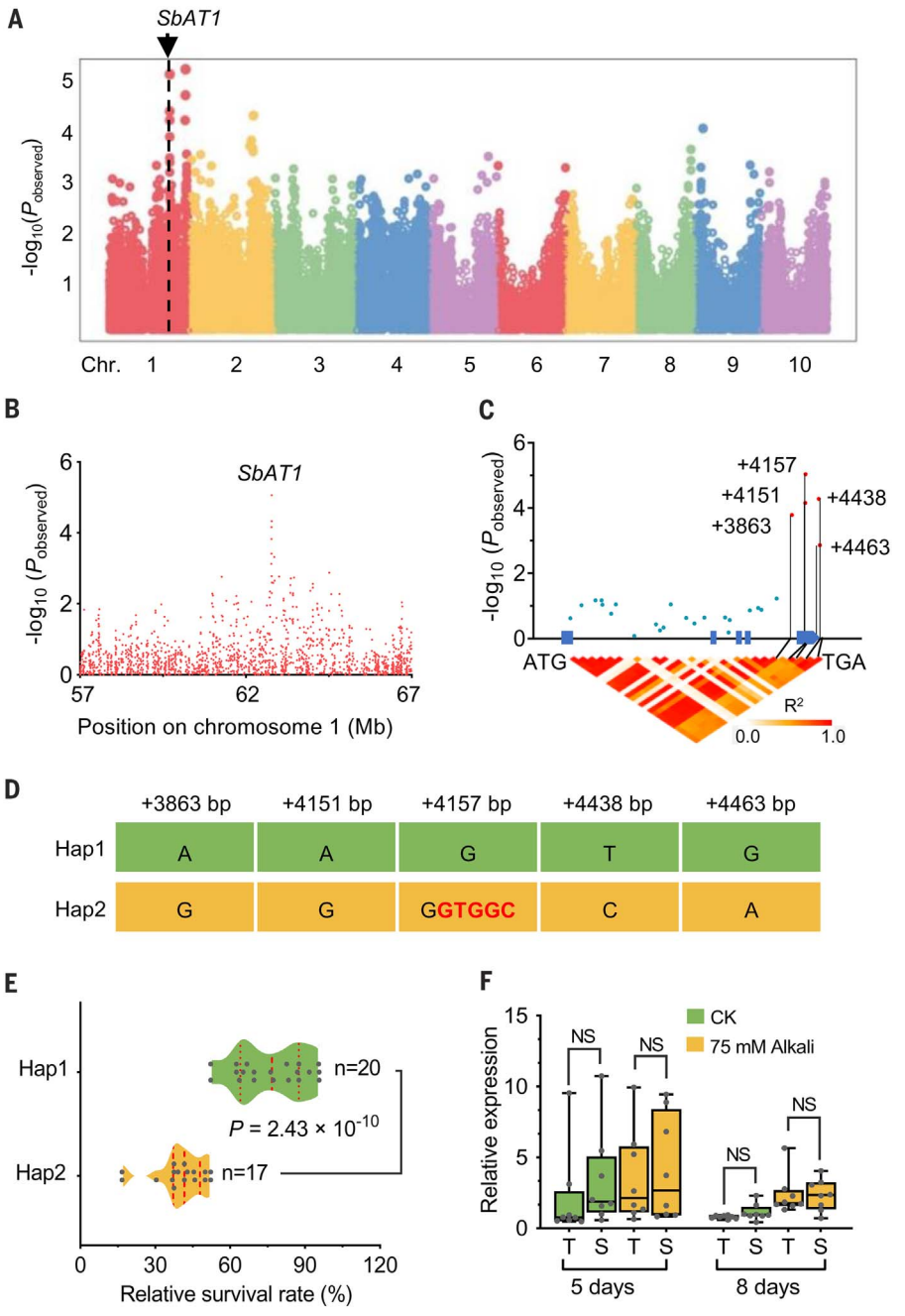

Fig. 1. Natural variation in *SbAT1* is associated with alkaline tolerance in sorghum. (**A**) Manhattan plot from a GWAS of alkaline tolerance in the natural sorghum association panel population. Relative survival rates were obtained from plants grown in conditions with (alkaline stress) or without (no-stress control) the addition of a 75 mM concentration of mixed alkali salts on the 21st day after seed sowing. The arrow identifies the major locus of *SbAT1*. (**B**) Scatter plot of the *SbAT1* locus flanked by an ~10-Mb genome region on chromosome 1. (**C**) *SbAT1*-based association mapping between the detected 29 sequence variations in the genic region of *SbAT1* and alkali tolerance among 37 sequenced sorghum accessions. LD analysis between the 29 causal sites indicates the linkage association signals. The five leading variant sites (red dots) show strong association signals with strong LD and are highlighted by black lines. (**D**) Two typical haplotypes (Hap1 and Hap2) of *SbAT1* were detected based on the five leading variant sites. A frame shift mutation (from "G" to "GGTGGC") within Hap2 is highlighted in red. (**E**) Relative survival rates of 20 sorghum accessions in Hap1 and 17 sorghum accessions in Hap2 subjected to alkaline stress (75 mM mixed alkali). Statistical *P* values were determined by two-tailed unpaired *t* test. (**F**) Relative expression levels of *AT1* in alkaline stress–tolerant (T) and –sensitive (S) lines ($n = 8$) after 5 and 8 days of stress in the 75 mM alkali treatment and the corresponding controls (CK). Statistical significance was determined by one-way ANOVA with Tukey's multiple comparisons test. NS, not significant.

classified into two typical haplotypes (Hap1 and Hap2) of *SbAT1*. Notably, compared with Hap1 [wild-type (WT)], we identified a frameshift mutation of a 5–base pair (bp) (GTGGC) insertion in the fifth exon of *SbAT1* (Fig. 1D), which resulted in a premature stop codon in Hap2 probably encoding a truncated protein with only 136 amino acids at the N terminus (named *Sbat1*). Furthermore, we observed that the sorghum accessions with Hap1 had much higher relative survival rates than those with Hap2 under the alkali treatment ($P = 2.43 \times 10^{-10}$) (Fig. 1E). Consistent with the finding that no strong association signals were found in the 5′ untranslated region (5′UTR) of *SbAT1*, we were able to confirm that haplotype-based variation was not associated with *SbAT1* expression levels on the basis of RNA levels obtained after 5 or 8 days of alkaline treatment (Fig. 1F). These data suggest that the alkali-sensitive and -tolerant phenotypes in the two *SbAT1* haplotypes are independent of the transcriptional levels of *SbAT1* and its variants but are instead due to the mutations leading to the protein changes inside the coding region.

The role of AT1 in alkaline tolerance

To assess the allelic effect of *AT1* on sorghum tolerance to alkali, we selected a pair of near-isogenic lines (NILs) with two *AT1* haplotypes in the F_{11} generation from our laboratory stock for breeding program (*18*). NILs were derived from a cross between two sorghum germplasms, SN010 and M-81E. SN010 was of the haplotype Hap1 (containing wild-type *SbAT1*) and showed higher alkaline tolerance than M-81E of the haplotype Hap2 (*Sbat1* mutant) according to our survival rate and plant height data (Fig. 2A and fig. S2, A to C). We treated the two NILs with 75 mM alkaline salt. NIL-*SbAT1* exhibited 56.1% higher relative survival rate and better growth than NIL-*Sbat1* under alkaline treatment, whereas the two NILs showed no significant difference when planted in neutral-pH soil (Fig. 2, B and C). The treatment with 75 mM mixed alkali salts imposed not only alkaline stress but also Na^+ stress on plants. To differentiate whether the *SbAT1*-related stress phenotype was caused by high pH or high Na^+ stress alone, we performed treatments similar to the alkaline treatments but with NaCl at 75-, 100-, 150-, and 200-mM concentrations and all soils at a neutral pH level. We found that both NILs were sensitive to high NaCl and there were only slight differences in stress responses between NIL-*SbAT1* and NIL1-*Sbat1* (fig. S2, D to F). This result indicates that the *SbAT1*- and *Sbat1*-related stress phenotype is more likely an alkaline-specific response rather than a salt-stress response.

To test this possibility, we generated additional transgenic sorghum plants in the Wheatland background (*Sb*WT) containing an intact wild-type *SbAT1* gene that was either overexpressed or knocked out using gene-editing technology. The overexpression or knockout (ko) was confirmed by quantitative reverse transcription polymerase chain reaction (RT-qPCR) or sequence analysis (fig. S2G) (*18*). Unexpectedly, we found that overexpression of *SbAT1* (*SbAT1-OE*) reduced tolerance, whereas plants with knockout of *SbAT1* (*SbAT1^{ko}*) showed greatly increased tolerance to alkalinity (Fig. 2, D to F, and fig. S2, H to J). *SbAT1*-overexpressing plants had a 13.95% lower survival rate than Wheatland plants under 75 mM alkaline stress, whereas *SbAT1^{ko}* plants had a 17.93% higher survival rate than *Sb*WT plants (Fig. 2F). The phenotype of the transgenic plants led us to reconsider the functionality of gene mutations in the *SbAT1* C terminus of natural varieties (Fig. 1, C and D) and to consider that a truncated protein may play a negative role in alkaline tolerance. To verify our speculation, we first transiently expressed the green fluorescent protein (GFP) fusion proteins SbAT1-GFP and Sbat1-GFP in plant cells and found that the protein accumulated to high levels (fig. S2K). This indicated that the mutated *Sbat1* gene could be translated (*18*).

To further investigate, we generated transgenic plants to create a stop codon at the same position as sorghum *at1* by gene editing in millet to mimic the production of a potential C-terminal truncated SiAT1^{102} protein. We also generated plants overexpressing SiAT1^{124} (*SiAT1^{124}-OE*) with a truncated C terminus and plants with *SiAT1* knockout (*SiAT1^{ko}*) (Fig. 3A and fig. S3, A and B). We used millet in this experiment for multiple reasons: (i) there is easier and faster plant transformation for millet compared with sorghum, (ii) millet is a close relative of sorghum with high genome similarity and similar environmental physiology, and (iii) the single copy of SiAT1 shares a 75.24% protein identity to SbAT1. Similar to the results with the transgenic sorghum, knockout of the *SiAT1* gene produced plants with greater tolerance to alkaline conditions, as observed in the higher survival rate compared with other genotypes (Fig. 3, B and C). By contrast, the transgenic millet with the

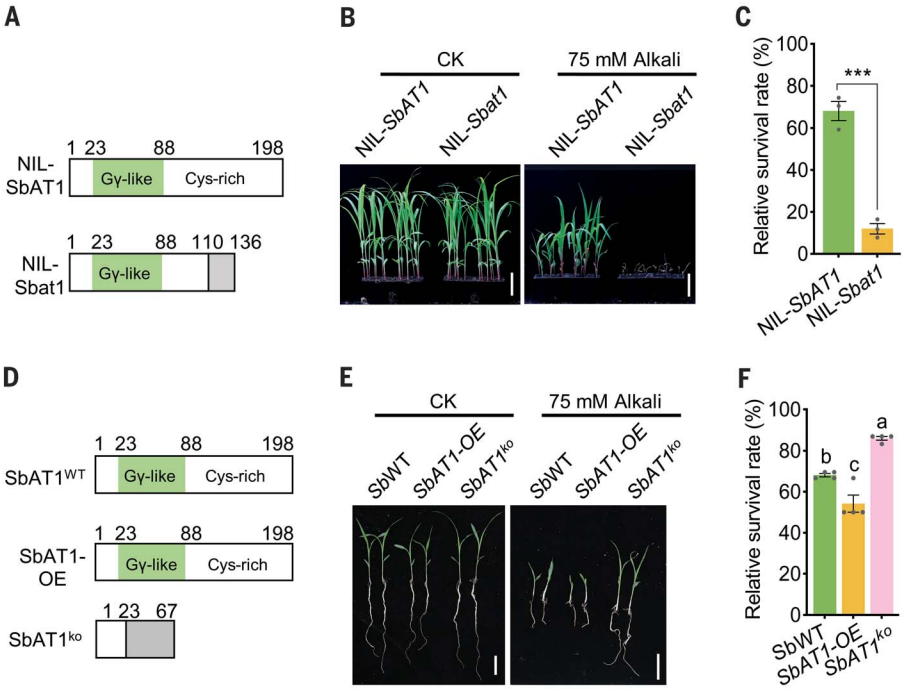

Fig. 2. *SbAT1* functions in alkaline tolerance in sorghum. (**A**) Schematic presentation of SbAT1 and its truncated protein Sbat1 in sorghum NIL-*SbAT1* and NIL-*Sbat1* plants. (**B**) Phenotypic analysis of sorghum NIL seedlings under alkaline stress. Seeds were sown in soil without (control, CK) or with 75 mM mixed alkali. Photographs were taken on the 14th day after seed sowing. Independent experiments were repeated three times. Scale bars, 5 cm. (**C**) Statistical analysis of the relative survival rates of seedlings in (B). Data are the means ± SEMs (n = 36 plants for each repeat) of three biological replicates. Statistical significance was determined by two-tailed unpaired t test. (**D**) Schematic presentation of SbAT1 and its nonfunctional version in *Sb*WT, *SbAT1-OE*, and *SbAT1^{ko}* plants. *Sb*WT is the Wheatland ecotype. (**E**) Representative seedlings of *Sb*WT, *SbAT1-OE*, and *SbAT1^{ko}* with or without 75 mM alkali stress treatment on the 14th day. Scale bars, 5 cm. (**F**) Statistical analysis of the relative survival rates of samples in (E). Data are the means ± SEMs (n = 16 plants for each repeat) of four biological replicates. Statistical significance was determined by ordinary one-way ANOVA with Tukey's multiple comparisons test.

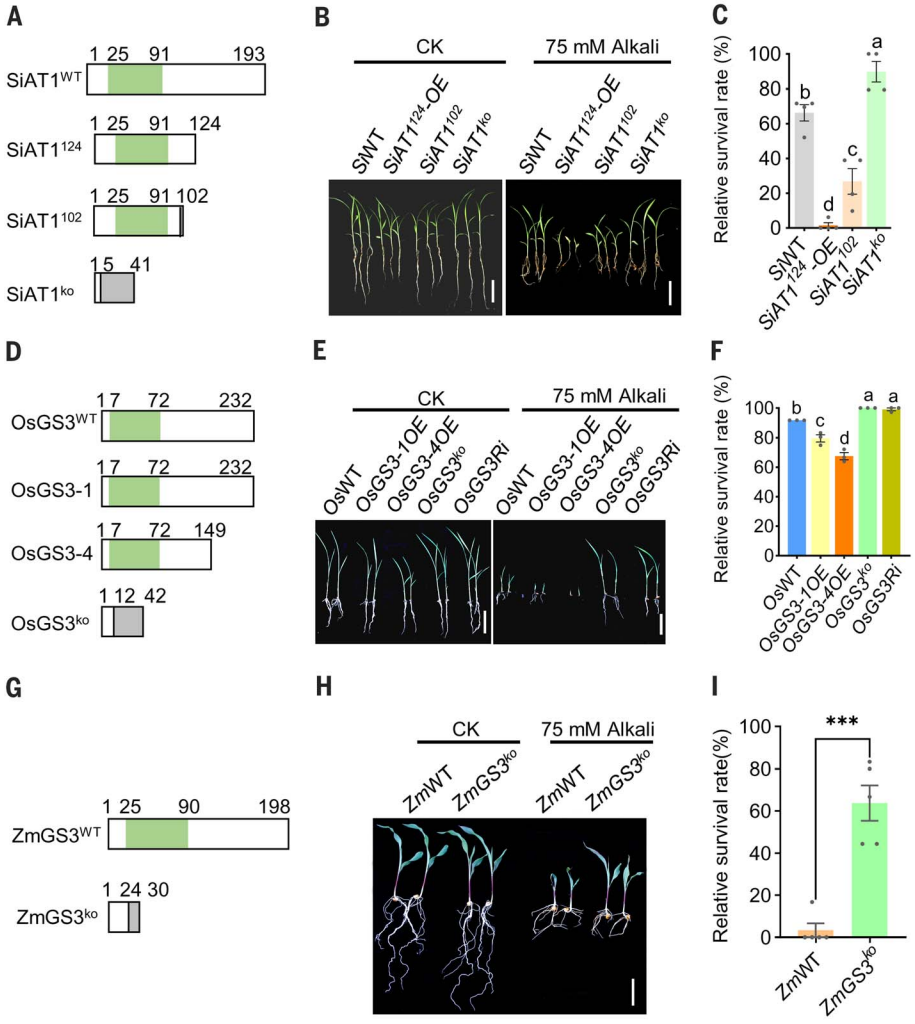

Fig. 3. The Gγ-like subunits of AT1 homologs have a conserved function in alkaline tolerance in millet, rice, and maize. (**A**) Schematic presentation of millet SiAT1 and its truncated or nonfunctional versions in *SiAT1* genetic plants. *Si*WT is the Ci846 ecotype. (**B**) Representative *SiAT1* genetic plants with or without 75 mM alkali stress on the 14th day. Scale bars, 5 cm. (**C**) Statistical analysis of the relative survival rates of millet lines in (B). Data are the means ± SEMs (n = 24 plants for each repeat) of three biological replicates. (**D**) Schematic presentation of rice OsGS3 and its truncated or nonfunctional versions in *OsGS3* genetic plants. *Os*WT is the ZH11 ecotype. (**E**) Representative seedlings of *OsGS3* genetic plants with or without 75 mM alkali stress on the 21st day after seed sowing. Scale bars, 5 cm. (**F**) Statistical analysis of the relative survival rate of rice lines in (E). Data are the means ± SEMs (n = 36 plants for each repeat) of three biological replicates. In (C) and (F), statistical significance was determined by ordinary one-way ANOVA with Tukey's multiple comparisons test. Different letters above the bars indicate significantly different groups. (**G**) Schematic presentation of wild-type ZmGS3 in *Zm*WT maize and its nonfunctional versions in *ZmGS3*^{ko} maize. *Zm*WT is the KN5585 ecotype. (**H**) Representative seedlings of *Zm*WT and *ZmGS3*^{ko} maize with or without 75 mM alkali stress treatment on the 14th day after seed sowing. Scale bar, 5 cm. (**I**) Statistical analysis of the relative survival rates of maize lines in (H) on the 50th day after seed sowing. Data are the means ± SEMs (n = 16 plants for each repeat) of four biological replicates. Significant differences were determined by two-tailed unpaired t test.

C terminus truncated (*SiAT1*^{102}) and the millet overexpressing the C terminus truncated SiAT1 (*SiAT1*^{124}*-OE*) showed reduced alkaline tolerance; *SiAT1*^{124}*-OE* plants exhibited the weakest growth in response to alkalinity (Fig. 3, B and C, and fig. S3C). This result suggests that the C-terminal truncated protein can be expressed in plants and that the increased amount of the C-terminal truncated protein had a negative effect on alkaline tolerance, whereas knockout of *AT1* could positively affect alkaline tolerance in plants. Together with the *AT1*-overexpression phenotype in sorghum, we conclude that AT1 plays a negative role, and at1 mutation enhances this role in alkaline tolerance in both sorghum and millet.

Similar roles of AT1 homologs in rice and maize

We further investigated the response of AT1 homologs in two other major monocot crops, rice and maize. The *AT1* ortholog in rice has been identified as *OsGS3*, a major quantitative trait locus (QTL) for grain size regulation (*16*, *19*). We found that in alkaline soils (75 mM alkaline salt; pH 9.0 to 9.2), overexpression of intact *OsGS3* (*OsGS3-1OE*) and a C-terminal truncated version (*OsGS3-4OE*) exhibited reduced alkaline tolerance, whereas rice with either a knockout (*OsGS3*^{ko}) or RNA interference of *OsGS3* (*OsGS3Ri*) showed greater tolerance in terms of relative survival rate, plant growth measured in relative plant height, and relative chlorophyll content compared with the ZH11 wild type (*Os*WT) (Fig. 3, D to F, and fig. S3, D to F). Among the transgenic plants, *OsGS3-1OE* and *OsGS3-4OE* exhibited 12.5 and 26.4% lower relative survival rates than *Os*WT, respectively, whereas *OsGS3*^{ko} and *OsGS3Ri* showed 8.3 and 7.4% higher relative survival rates than *Os*WT, respectively (Fig. 3F). These results demonstrated that inhibition of *OsGS3* function in rice could enhance alkaline tolerance and suggested a conserved function of the Gγ subunit. Moreover, by manipulating or selecting nonfunctioning alleles of *OsGS3*, we could enhance alkaline tolerance in rice.

The maize ortholog of *AT1* was previously identified as *ZmGS3* (*17*). We thus designate this gene as *AT1/GS3*, with a prefix to specify the species; *AT1* and *GS3* may also be separately or interchangeably used, depending on the context. We generated maize *ZmGS3* knockout (*ZmGS3*^{ko}) lines through gene editing in the maize line KN5585 (*Zm*WT). The maize *ZmGS3*^{ko} plants had a 34-bp deletion and a base mutation occurring in the first exon of *ZmGS3*. These mutations resulted in a frame shift and early translational termination of the predicted protein (fig. S3G). Upon alkaline treatment, the knockout plants appeared to have enhanced alkaline tolerance, as indicated by growth performance at day 14 of cultivation, compared with the wild type (Fig. 3, G and H, and fig. S3H). Differences in phenotypes were more marked after 50 days of treatment; almost all the wild-type seedlings died, whereas the *ZmAT1/GS3*^{ko} survived and continued to grow (Fig. 3I and fig. S3I). This evidence supports that *ZmAT1/GS3*^{ko} could also increase alkaline tolerance in maize, similar to what we observed in sorghum, millet, and rice.

AT1/GS3 cooperates with aquaporins

To further ascertain how AT1/GS3 regulates crop alkaline tolerance, we detected SbAT1-interacting proteins by immunoprecipitation in combination with mass spectrometry

(IP-MS). Glutathione S-transferase (GST)–SbAT1 was applied to bind proteins in alkaline-treated root samples, and then those bound proteins were released for further analysis. There were 386 proteins detected as candidates interacting with SbAT1 (table S2), including the guanine nucleotide–binding protein β subunit (Gβ subunit) (Fig. 4A), which supports the IP-MS result because it is well known that Gβ and Gγ function together in a complex to regulate a wide range of biological processes (*20*–*22*). A number of aquaporins, especially the PIP2;1/2;2 and PIP1;3/1;4 proteins, were found among the interacting proteins. Homologs of these aquaporins have been reported to be involved in stress biology by regulating ROS homeostasis in both plants and mammals (*12*, *23*). We confirmed the interactions of these proteins with both SbAT1 and Sbat1 by performing different assays. The luciferase complementation imaging (LCI) assay data together with the coimmunoprecipitation (Co-IP) assay and pull-down assay all demonstrated their interactions both in vivo and in vitro (Fig. 4, A and B, and fig. S4, B and C).

The rice aquaporin OsPIP2;1 shares high sequence similarity with its sorghum counterpart, and we also confirmed the interaction between OsPIP2;1 and OsGS3 (fig. S4D). We thus examined the function of OsPIP2 in the alkaline stress response. To investigate the roles of *OsPIP2;1* and its homolog *OsPIP2;2*, we generated a double knockout mutant of *OsPIP2;1* and *OsPIP2;2* using CRISPR-Cas9. Two independent T_2 homozygous lines with knockouts of both *OsPIP2;1* and *OsPIP2;2* (*OsPIP2;1*^{ko}/*2;2*^{ko}-8-3 and *OsPIP2;1*^{ko}/*2;2*^{ko}-9-8) were selected for further analysis (fig. S4, E and F). As shown in Fig. 4, C and D, *OsPIP2;1*^{ko}/*2;2*^{ko} had lower alkaline tolerance, as illustrated by their poorer relative survival rates and plant growth, compared with the respective control in rice. Because aquaporins are known to be involved in the homeostasis of ROS in cells across different life kingdoms (*12*, *24*) and plant root growth inhibition under alkaline stress is closely associated with ROS accumulation (*6*), we measured ROS accumulation by 2′,7′-dichlorodihydrofluorescein diacetate (H_2DCFDA) staining in rice roots. The fluorescent signal of H_2DCFDA staining reflects the ROS contents in plant tissues (*25*). The strong signal confirmed the higher ROS contents in plant roots of *OsPIP2;1*^{ko}/*2;2*^{ko} lines compared with the wild-type control line subjected to alkaline treatment (Fig. 4, E and F). These results suggest that aquaporins *PIP2;1/2;2* are involved in the regulation of alkaline tolerance by affecting the ROS status in plants. Because PIP2;1/2;2 interact with Gγ, we then measured the ROS accumulation of different transgenic lines of both sorghum and rice. Overexpression of *AT1/GS3* or the C-terminal truncated protein enhanced ROS accumulation in the roots of sorghum and rice compared with that of their respective controls, whereas knockout of *AT1/GS3* greatly reduced ROS accumulation (Fig. 4, G to J). The strong fluorescent signal staining also confirmed the higher ROS contents in plant roots of NIL-*Sbat1* compared with NIL-*SbAT1* after alkali treatment (fig. S5A).

We also analyzed ROS status in the leaves of transgenic sorghum, millet, rice, and maize that either overexpressed *AT1/GS3* or had a knocked out *AT1/GS3* together with sorghum NIL lines by 3,3′-diaminobenzidine (DAB) staining. DAB staining detected a brown precipitate in tissues, and the intensity of the staining was indicative of the amount of H_2O_2 accumulation. The DAB staining results in all

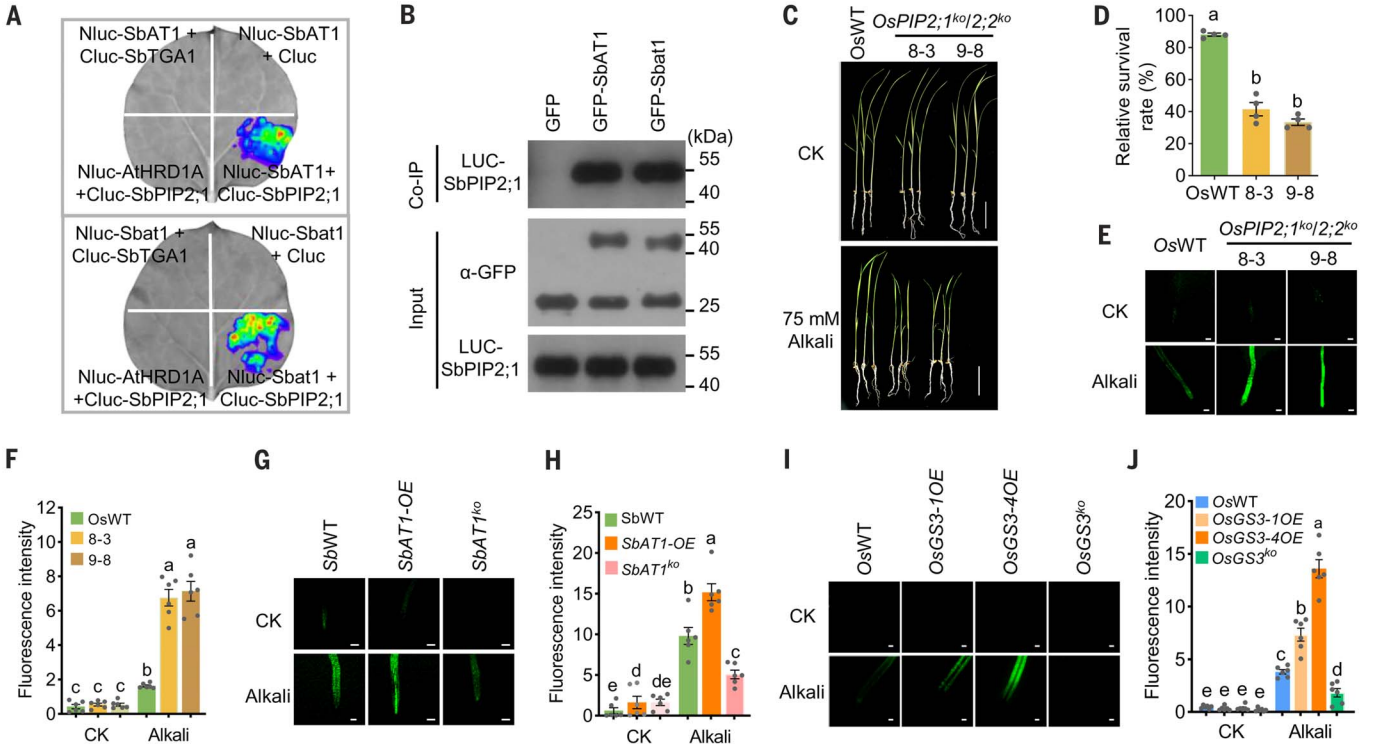

Fig. 4. The Gγ subunit AT1 interacts with aquaporin PIP2;1, which functions in plant alkaline tolerance. (**A**) LCI assay of both SbAT1 and Sbat1 with SbPIP2;1. Cluc-SbTGA1 and Nluc-AtHRD1A were used as the negative controls. (**B**) Co-IP assay of SbAT1 and Sbat1 with SbPIP2;1. (**C**) Phenotypic analysis of *OsPIP2;1*^{ko}/*2;2*^{ko} mutants under alkaline stress. Seeds of *Os*WT and two independent *OsPIP2;1*^{ko}/*2;2*^{ko} lines were sown in soil without (CK) or with 75 mM alkali. Photographs were taken on the 27th day after seed sowing. Scale bars, 5 cm. (**D**) Statistical analysis of the relative survival rates of plant materials, as in (C). Data are the means ± SEMs (n = 16 plants for each repeat) of four biological replicates in each treatment. (**E**, **G**, and **I**) H_2O_2 amount detection by an ROS detection probe (H_2DCFDA) in the root tips of *PIP2;1* and Gγ subunit–related genetic plants. Two-week-old sorghum and rice seedlings treated with or without 200 mM alkali for 48 hours were used for analysis. Scale bars, 100 μm. (**F**, **H**, and **J**) Statistical analysis of the H_2O_2 concentration in (E), (G), and (I). Data are the means ± SEMs (n = 6 plants). In (D), (F), (H), and (J), statistical significance was determined by ordinary one-way ANOVA with Tukey's multiple comparisons test.

four crops (fig. S5, B to F) confirmed the results of H_2DCFDA staining. It is well known that alkaline stress can cause ROS accumulation (*6*). Excessive amounts of ROS result in cellular oxidative stress, which causes cell death in plants and consequently reduces plant survival rates. The regulation of cellular ROS accumulation might explain why the truncated Gγ had lower survival rates and why the knockout of Gγ increased alkaline tolerance in these crops.

Gγ regulates PIP2 phosphorylation in ROS distribution

To further study how Gγ interacts with PIP2 aquaporins to affect ROS homeostasis in response to alkaline stress, we applied the redox probe Cyto-roGFP2-Orp1, which senses H_2O_2 in the cytoplasm (*26*–*28*). Fluorescence after excitation was observed at 405 and 488 nm but not in the no-plasmid control group (fig. S6A), which indicated that we successfully expressed the Cyto-roGFP2-Orp1 probe in rice protoplasts. We next analyzed the redox state of protoplasts overexpressing Cyto-roGFP2-Orp1 under different redox challenges. The morphology of the protoplast was complete, and fluorescence was not quenched under 100 μM dithiothreitol (DTT) or 100 μM H_2O_2. Protoplasts overexpressing Cyto-roGFP2-Orp1 responded well to reductive challenge and oxidative challenge, and the response range (ratio of oxidation:reduction) was 2.9 (Fig. 5, A and B), which is within the dynamic range of the roGFP2-Orp1 probe reported (*29*). These results showed that this system is suitable for the detection of redox in rice protoplasts.

Next, we performed the assay under alkaline treatment conditions. The standard pH for rice protoplasts is 5.4, and we found that the highest pH under which the protoplasts can still remain intact after a certain treatment time was 7.5. Then, we treated the wild-type protoplast with this alkaline condition for different time points and observed cell integrity. Imaging results showed that the protoplasts remained intact at pH 7.5 for 40 min, but rupture of the protoplast was observed after 60 min of alkali treatment (as shown by the blue arrow in fig. S6B, left panel). We also found that the H_2O_2 level at 40 min was markedly higher than that of the control but was not induced at 20 min under the alkali treatment compared with CK buffer (pH 5.4) treatment. Therefore, we selected the 40-min time point as the appropriate treatment condition (fig. S6B, right panel).

We then used this Cyto-roGFP2-Orp1 system and the treatment conditions to detect redox status in the protoplasts of *Os*WT, *OsGS3-4OE*, *OsGS3*^{ko}, and *OsPIP2;1*^{ko}*/2;2*^{ko} lines. The results showed that the relative H_2O_2 level increased upon alkaline treatment compared with their untreated controls, and representative cells are shown in fig. S6C based on $n > 30$ protoplasts analyzed in each group. To overcome the variation in individual protoplasts, we measured the redox states in large numbers of cells (with 1×10^5 protoplasts each repeat) of those same lines transfected with Cyto-roGFP2-Orp1 at 525 nm after excitation at 405 and 488 nm detected by a microplate reader. As shown in Fig. 5C, after alkaline treatment, the relative H_2O_2 levels were higher in the *OsGS3-4OE* group than in the *Os*WT. These results suggested that *OsGS3-4OE* performed negatively in the alkali response because of the production of high H_2O_2 in cells, whereas lower ROS accumulation in *OsGS3*^{ko} could be one of the reasons why *OsGS3*^{ko} is tolerant to alkaline treatment. We also observed that the relative H_2O_2 levels were significantly higher in *OsPIP2;1*^{ko}*/2;2*^{ko}-8-3 compared with *Os*WT under alkali treatment (Fig. 5D).

Previous studies on PIP2;1 in *Arabidopsis* have found that modifications in the phosphorylation of PIP2;1 affect its activity (*30*, *31*). Thus, we studied the function of SbPIP2;1 phosphorylation on ROS distribution under alkaline stress. First, we identified phosphorylation sites in SbPIP2;1 by liquid chromatography with tandem mass spectrometry (LC-MS/MS) in seedling samples treated or untreated with alkaline stress and detected two phosphorylation sites, S285 and S288 (fig. S6D). We found that overexpression of *SbAT1* could attenuate the phosphorylation of SbPIP2;1 (Fig. 5E). Using the anti-pS285/288 antibody, we quantified the phosphorylation levels of OsPIP2;1 in rice *OsGS3* transgenic lines grown in the control and alkali treatment conditions. The phosphorylation levels of OsPIP2;1 in both lines overexpressing the full-length *OsGS3* (*OsGS3-1OE*) and the short form of *OsGS3* (*OsGS3-4OE*) were lower than the level in the wild-type control, whereas the phosphorylation levels of OsPIP2;1 were higher in *OsGS3*^{ko} (Fig. 5F), which is similar to what we found in sorghum PIP2;1 (Fig. 5E). These results suggested that AT1/GS3 might modulate ROS homeostasis in plants by attenuating the phosphorylation of PIP2;1 when stressed by alkaline conditions.

To confirm our observation of the phosphorylation of PIP2;1 on the cellular ROS status in plant cells, we transiently expressed a fusion construct in the protoplast of the rice *OsPIP2;1*^{ko}*/2;2*^{ko} mutant by inserting a P2A self-cleaving peptide (*32*) in the region between different phosphorylation forms of OsPIP2;1 and the ROS probe (Cyto-roGFP2-Orp1), which could produce two equal molar proteins of OsPIP2;1 and the ROS probe (Fig. 5G). As shown in Fig. 5H, there was no significant difference in untreated cells, but the higher ROS production in cells was repressed by overexpression of *OsPIP2;1* in the *OsPIP2;1*^{ko}*/2;2*^{ko} mutant. Additionally, the phosphorylated form of OsPIP2;1(3SD) effectively attenuated the ROS level, whereas the dephosphorylated form of PIP2;1 (3SA) accumulated higher ROS levels in cells upon alkali treatment (Fig. 5H). These results indicate that Gγ negatively regulates the phosphorylation of PIP2;1, leading to elevated ROS levels in plants.

To further reveal how PIP2s and AT1/GS3 function in the control of cellular ROS levels under stress conditions, we detected and quantified the relative ROS content in both cytosol and apoplast in the root tissues of rice lines, such as wild-type ZH11, *OsGS3-4OE*, *OsGS3*^{ko}, and *OsPIP2;1*^{ko}*/2;2*^{ko}-8-3 lines, by staining with H_2DCFDA (cytosolic redox status) and OxyBURST Green H_2HFF BSA (apoplastic redox status) upon alkaline treatment. We found very little difference in the ROS content in all of these rice lines without alkaline treatment (Fig. 5, I to L). After alkali treatment, significantly increased cytosolic ROS accumulation was detected in *OsGS3-4OE*, whereas cytosolic ROS accumulation was reduced in *OsGS3*^{ko} compared with the wild-type control (Fig. 5, I and J). We also examined the apoplastic ROS level of the same lines. *OsGS3-4OE* showed relatively lower-apoplast ROS than *Os*WT, whereas high-apoplast ROS accumulation was detected in the roots of the *OsGS3*^{ko} line. Increased cytosolic ROS and reduced apoplastic ROS accumulation were also detected in *OsPIP2;1*^{ko}*/2;2*^{ko} compared with ZH11 (Fig. 5, I to L). These results revealed that the G protein γ subunit GS3/AT1 and aquaporin OsPIP2;1/2;2 could function in opposite ways to regulate the cytosolic/apoplast ROS ratios in response to alkaline stress in plant roots. Together with cytosol ROS detected by the ROS probe (Cyto-roGFP2-Orp1), these results suggest that GS3/AT1-mediated phosphorylation of OsPIP2 aquaporins might function to regulate intracellular ROS levels and avoid damage to plant roots under alkaline stress.

Enhanced field crop yield in highly sodic lands

To assess the usefulness of the *AT1/GS3* gene for crop production, we field tested sorghum, rice, maize, and millet with different natural alleles and genetically modified *AT1/GS3* genes in highly sodic lands containing natural alkali. The fields are located in two sites within sodic regions in China—the Daan region in Jilin Province (northern China) and the Pinglou region in Ningxia Province (northwestern China). These regions are among the main crop production areas in China but have large areas of sodic soils, which limit crop production.

KY^{NIL}(*GS3*) is the elite cultivar Kongyu131 carrying *OsGS3-2* (with an in-frame 3-bp insertion in the C terminus relative to *OsGS3-1*), which is functionally equivalent to *OsGS3-1*. KY^{NIL}(*gs3*$^{-}$) is in the background of Kongyu131 with an introgressed *OsGS3-3*, which is a complete loss-of-function allele. Before the field

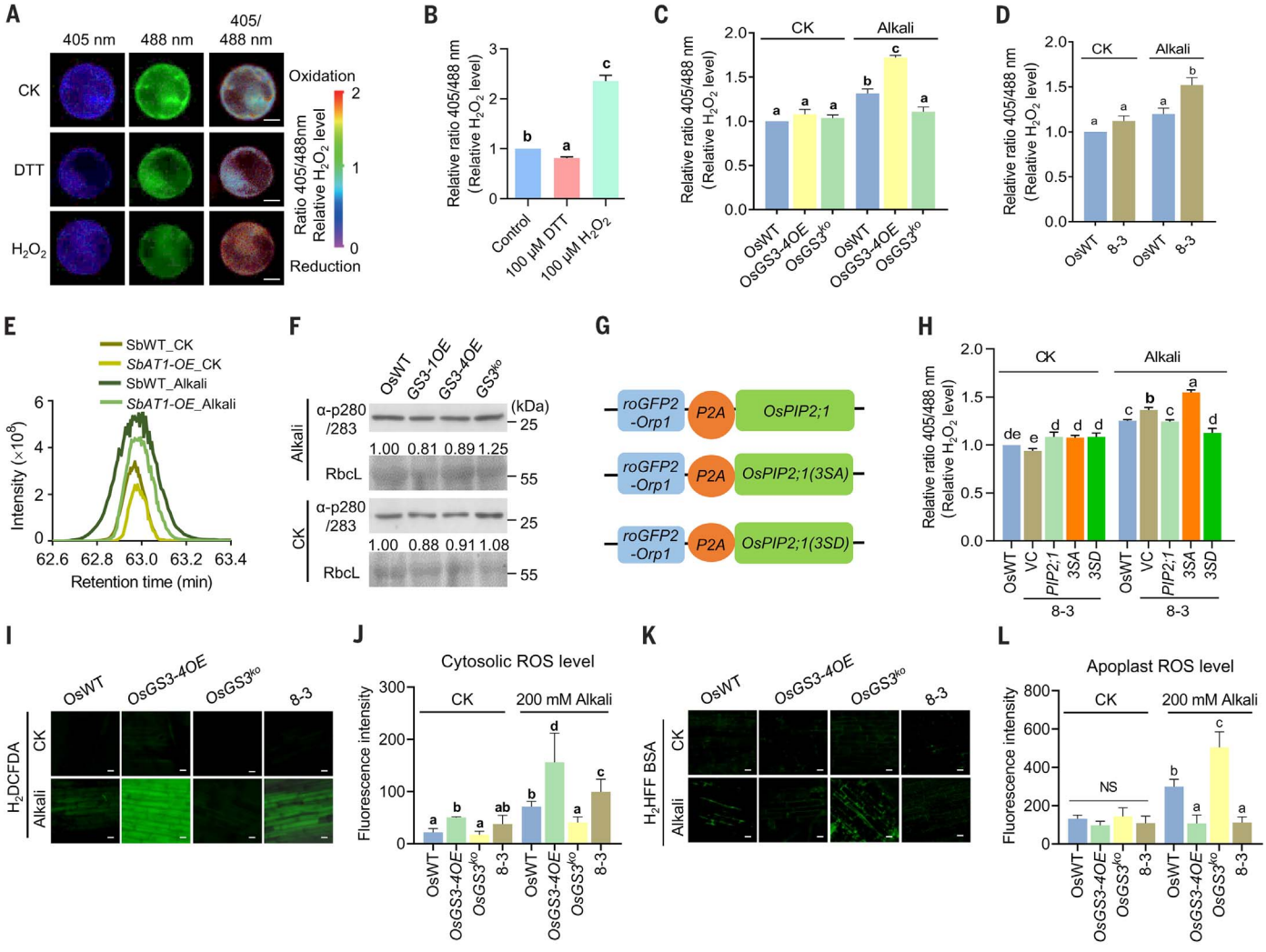

Fig. 5. The Gγ subunit of AT1 homologs regulates the plant alkali response through the H_2O_2 exporter PIP2;1. (**A**) Confocal imaging of Cyto-roGFP2-Orp1 in *Os*WT protoplasts treated with 100 μM DTT and 100 μM H_2O_2 separately. Scale bars, 5 μm. (**B**) The relative 405/488 nm ratio of Cyto-roGFP2-Orp1 in samples measured with a microplate reader. (**C** and **D**) Detection of cytosolic H_2O_2 accumulation in the Gγ subunit and *PIP2;1*-related genetic plants. The protoplasts transfected with Cyto-roGFP2-Orp1 were treated with standard W5 liquid (pH 5.54, CK) or W5 liquid by the addition of alkali to pH 7.5 (Alkali) for 40 min. 8-3, *OsPIP2;1^{ko}/2;2^{ko}*-8-3. (**E**) Relative abundance of the phosphopeptides, including S285 and S288 sites, by LC-MS/MS. *Sb*WT and *SbAT1-OE* plants were treated with or without 75 mM alkali. (**F**) OsGS3 affects the phosphorylation level of OsPIP2;1. Three-day-old rice plants treated with 200 mM alkali for 6 hours were subjected to phosphorylation analysis with an α-p280/283 antibody. The large subunit of ribulose-1,5-bisphosphate carboxylase/oxygenase (RbcL) was used as a loading control. (**G**) Schematic diagram of *roGFP2-Orp1-P2A-OsPIP2;1/OsPIP2;1 (3SA)/OsPIP2;1(3SD)* fusion genes used in (H). (**H**) Phosphorylation of OsPIP2;1 is essential for its function in modulating H_2O_2 accumulation in the cytosol. VC, vector control. *3SA*, *OsPIP2;1(3SA)*; *3SD*, *OsPIP2;1(3SD)*. In (B) to (D) and (H), data are the means ± SEMs (three replicates, ~1 × 10^5 cells of each line in each replicate). (**I** and **K**) Cytosol and apoplast ROS in situ detection of *Os*WT, *OsGS3-4OE*, *OsGS3^{ko}*, and *OsPIP2;1^{ko}/2;2^{ko}*-8-3 plants. Scale bars, 20 μm. (**J** and **L**) Statistical analysis of H_2O_2 accumulation in (I) and (K). Data are the means ± SEMs ($n \geq 8$). In (B) to (D), (H), (J), and (L), statistical significance was determined by ordinary one-way ANOVA with Tukey's multiple comparisons test.

trial, the alkaline tolerance of KY^{NIL}(*GS3*) was tested in comparison with KY^{NIL}(*gs3*$^-$). The test was carried out at the seedling stage in a greenhouse with 75 mM alkali. As expected, KY^{NIL}(*gs3*$^-$) showed much higher alkaline tolerance than Kongyu131 (fig. S7, A and B).

We then conducted an experiment to compare NILs in soils with two different pH values, 9.45 and 7.74 (control), using highly sodic soils from the same region mixed with nutrient soil. Except for the number of panicles per plant (fig. S7C), KY^{NIL}(*gs3*$^-$) showed significantly better performance than KY^{NIL}(*GS3*) in relative survival rate, the number of grains per panicle, grain weight, and grain yield (fig. S7C) under sodic soil with pH 9.45.

We also performed a field test with a designed plot experiment in Daan, where the soil pH was 9.17. The KY^{NIL}(*gs3*$^-$) line performed much better than KY^{NIL}(*GS3*) at both the seedling (fig. S7D) and harvest stages (Fig. 6A, left panel), indicating enhanced alkaline tolerance in KY^{NIL}(*gs3*$^-$). At the harvest stage, KY^{NIL}(*gs3*$^-$) rice produced larger panicles (fig. S7E) with a higher number of grains per panicle (Fig. 6A, third panel) and increased grain weight (Fig. 6A, fourth panel), resulting in a 29.3% increase in grain yield per clump (Fig. 6A, fifth panel). The grain yield was 27.8% higher for the KY^{NIL}(*gs3*$^-$) rice compared with the control (Fig. 6A, right panel).The same plantings were established in a field with a pH of 5.58, where the difference in yield per plant between

KY^{NIL}(*gs3*$^{-}$) and the control was only 10.3% (fig. S7F). The grain yield of the rice NILs in sodic soil and acidic soil was studied in the same location on the second year. There was a 22.4% yield increase in alkaline soil and a 6.64% increase in the control field (fig. S7, G and H), similar to results obtained previously. Furthermore, *OsGS3* knockout contributed to grain length in both sodic soil and neutral soil. We also found that *OsGS3* knockout contributed to width in sodic soil but not in neutral soil (fig. S7, I and J). These results show that the nonfunctional allele of *GS3* could achieve higher crop production in highly sodic soils.

Because of its good quality and high yield, the improved elite rice line Zhongkefa5 (ZKF5) has been planted in >0.1 million ha in northern China since 2018. ZKF5 has a nonfunctional allele of *GS3* (*OsGS3-3*), similar to that in KY^{NIL}(*gs3*$^{-}$). We tested ZKF5 field performance in relatively high-sodic soil (pH 8.5 to 8.7) and low-sodic soil (pH 7.4 to 7.6) in the summer of 2021. At the end of the growing season, field production data were obtained from >30 ha of land by the local farmer association. We found only a 7.8% reduction in yield production in the sodic field when compared with that in the neutral field (fig. S7K). These large-area field production data also indicate the potential for increasing crop production by using the *GS3-3* allele in rice production in sodic lands.

We also planted Zhonghua 11 (ZH11) rice and its *OsGS3* knockout line, *OsGS3*^{ko}, in soils of the same two pH levels—7.74 as the control and 9.45 as the sodic soil—in a greenhouse. Although we failed to harvest the seeds of ZH11 because of its photoperiod sensitivity when planted in Jilin Province, the greater relative survival rate observed in the *OsGS3*^{ko} line (fig. S7L) demonstrates its greater tolerance to sodic conditions.

Sorghum, maize, and millet were tested in the Pingluo region, which consists of dry lands with highly sodic soil in northwestern China. In this region, the pH naturally increases during the crop growing season because of changes in the underground water level (*2*). The Wheatland wild-type and *SbAT1*^{ko} lines of sorghum were planted in the same plot with a pH of 8.97 in the spring season that reached a pH of 9.27 at the flowering stage in August. The survival rate was >60% for the *SbAT1*^{ko} line and only 33% for the Wheatland wild-type control (Fig. 6B, first and second panels). Leaf burn, a symptom that usually occurs in monocotyledonous crops affected by high salt or sodic stress, was observed in most Wheatland wild-type plants but not in plants of the *SbAT1*^{ko} line (Fig. 6B, first panel). At the harvest stage, the grain yield of the *SbAT1*^{ko} line was 20.1% greater than that of the control (Fig. 6B, third panel) despite its lower numbers of tillers and panicles (Fig. 6B, fourth and fifth panels). Because whole sorghum plants are commonly used for silage, we measured the fresh weight of whole-plant biomass and found that the fresh weight of plants in the *SbAT1*^{ko} line was 30.5% higher than that of the control (Fig. 6B, right panel). Both the higher grain production and whole-plant biomass of the *SbAT1*^{ko} line compared with those of the wild type demonstrated greater field performance for sorghum grown in sodic land. In the same region, we also planted the NIL-*SbAT1* and NIL-*Sbat1* lines in the summer season. At the end of August, we found that NIL-*SbAT1* outperformed NIL-*Sbat1* (Fig. 6C), and the differences were similar to the results recorded from the greenhouse experiment (Fig. 2B).

The *SiAT1*^{ko} line and its control, Ci846, were also planted together with sorghum in the same region. The *SiAT1*^{ko} line at the seedling stage had a survival rate of nearly 100%, whereas the wild-type Ci846 had a survival rate of only 75% (Fig. 6D, left panel). Additionally, at the harvest stage, the panicle size of the knockout line was also larger than that of the control (Fig. 6D, middle panel), and the grain yield of *SiAT1*^{ko} was 19.5% higher than that of the control (Fig. 6D, right panel).

In the same field, we also planted maize with *ZmGS3* knocked out together with its control line KN5585 (*Zm*WT). At the seedling stage, the *ZmGS3*^{ko} line showed a relative survival rate of 42.5% compared with 18.5% of the wild-type control, as recorded 1 month after planting (Fig. 6E). After 3 months of growth, most individuals of the KN5585 line died, whereas 7.4% of individuals from the knockout line survived. Although none of these plants reached maturity to produce grains because of the inherent sensitivity of maize to alkaline conditions, knockout of *ZmGS3* showed enhanced alkaline tolerance. Altogether, we conclude that nonfunctional mutants, either obtained from natural variations or generated by gene editing, can improve the field performance of crops in terms of biomass or grain production when cultivated in sodic soils.

Discussion

In this study, we have identified and demonstrated that natural alleles of AT1, an atypical G protein γ subunit, contribute to alkaline tolerance in four different monocotyledonous crops. The N-terminal domain of AT1 and its homologs played negative roles in alkaline stress tolerance. Crops with a truncated protein were highly sensitive to alkaline stress. This might be because of the inhibitory role of the C-terminal domain, which is necessary for protein degradation in its rice homolog (*33*, *34*). Accordingly, overexpression of the entire protein results in higher sensitivity to alkaline stress due to higher amounts of the protein, and overexpression of the truncated protein leads to an even higher sensitivity to alkaline stress. By contrast, high tolerance to alkalinity was observed in the knockout or natural variants with nonfunctional alleles in all four crops because of a lack of the N-terminal domain (Fig. 6F).

SbAT1 and *OsGS3* play pleiotropic roles in agronomic trait regulation and stress response (*35*, *36*). Both *OsGS3* and *SbAT1/qTGW1a* are key determinants of grain size (*19*, *37*). *OsGS3* also participates in stigma exsertion (*38*). Additionally, we found that *SbAT1*, previously also named *GC1* (*Glume Coverage 1*) because of its role in regulating sorghum glume coverage (*18*), affects alkaline tolerance in monocot crops (sorghum, rice, maize, and millet). *OsGS3* is also involved in salinity and chilling stress with an unknown mechanism (*36*) and controls thermotolerance in rice through alteration of wax biosynthesis (*39*). Accordingly, SbAT1 and OsGS3 act as negative regulators of these traits, and the truncated proteins with only an N-terminal domain led to a reduced grain size and low glume coverage. Because G protein γ subunits play important roles at the early stages of cell signaling pathways, it is not a surprise that they have pleiotropic effects in different aspects of plant development and stress tolerance. Nevertheless, the identification of the downstream components of the G protein is an important aspect in plants. We also note the need to consider the probable negative effect of nonfunctional alleles of *SbAT1/GC1* for sorghum due to the production of longer glume sizes (*18*), which might be unfavorable for threshing. For rice, slightly higher plant height was observed in the knockout mutant and natural nonfunctional mutant of *OsGS3* (*33*), and this characteristic might not be favored by breeders.

Cells have developed different systems to protect themselves by activating metabolic pathways involving ROS or peroxiporins to facilitate H_2O_2 export from cells and maintain homeostasis. Aquaporins have no catalytic activity to convert oxidative species to less harmful molecules in cells, but aquaporins are known to be involved in bidirectional transport of oxidative species in cells. Most transport assays were performed with additions of excess amounts of extracellular H_2O_2 to demonstrate the ability of transporters to import H_2O_2 across the cell membrane. However, when genes encoding the H_2O_2-degrading enzyme glutathione peroxidase (GPX1) or catalase (CAT) are knocked out, the excess amount of H_2O_2 present in stressed cells can be exported with the assistance of certain aquaporins that function as peroxiporins to detoxify the cell (*9*). We found a similar function in plant aquaporins in the regulation of the ROS level under stress after we investigated mutants with a knockout of *OsPIP2;1* that overexpressed both sorghum and rice aquaporins. Overall, these results highlight the important

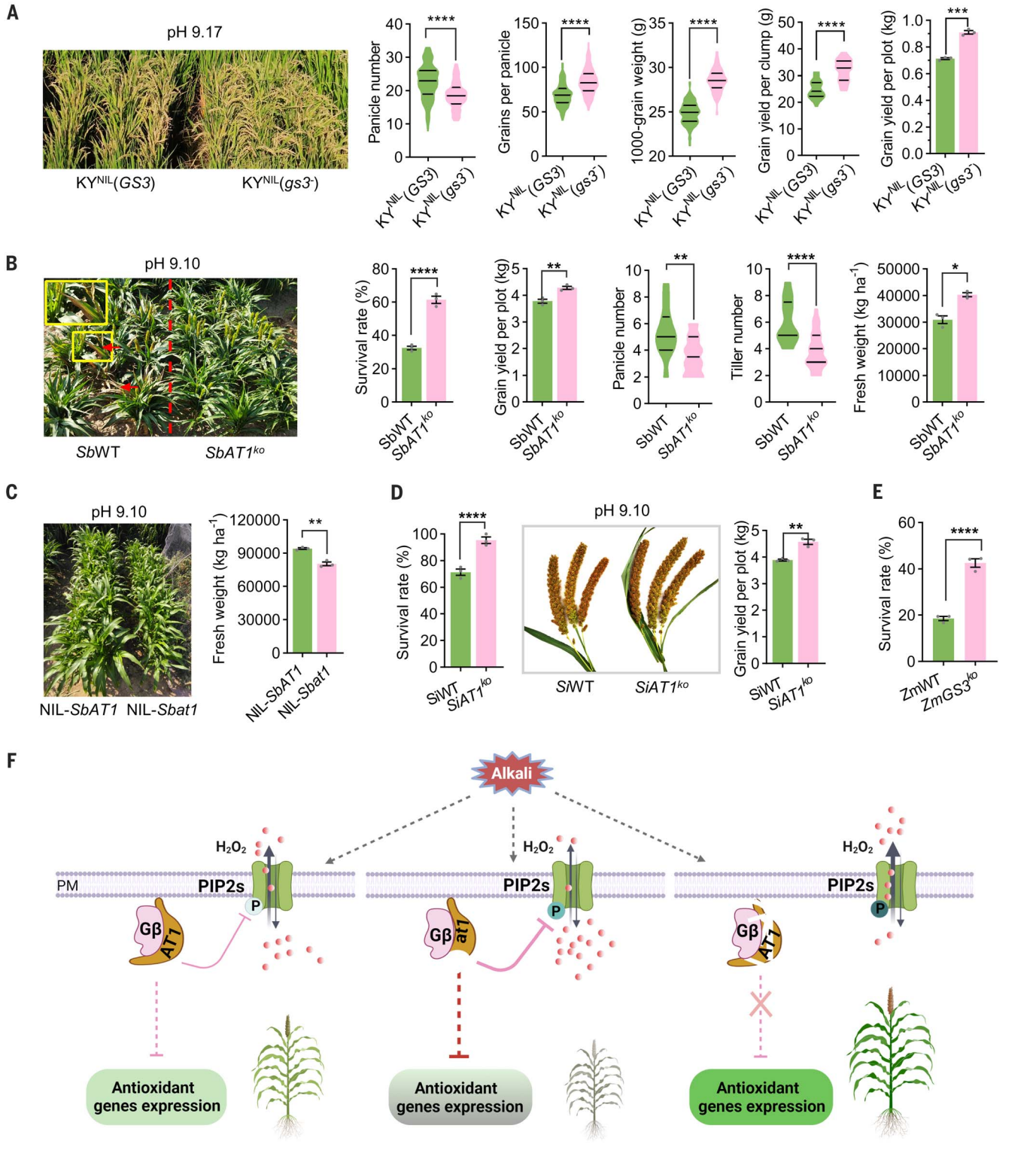

Fig. 6. *AT1/GS3* knockout and natural nonfunctional alleles enhance crop yield in saline-alkaline fields. (**A**) Phenotype and grain production of rice KY^{NIL}(*GS3*) and KY^{NIL}(*gs3*$^{-}$) from the alkali field (pH 9.17) in Jilin Province, China, in 2021. The first panel shows the phenotype of the rice plants at the reproductive stage (3 months after planting in the field). The panicle number indicates the number of panicles per plant. Data are the means ± SEMs (*n* = 3 plots). (**B**) Phenotype, survival rate, grain production, and whole biomass of *Sb*WT and *SbAT1*^{ko} grown in the alkali field (pH 9.10) of Ningxia Province, China, in 2021. Data are the means ± SEMs (*n* = 3 plots). (**C**) Phenotype and fresh weight of NIL-*SbAT1* and NIL-*Sbat1* seedlings grown in the alkali field (pH 9.10) of Ningxia Province, China, in 2021. (**D**) Phenotype, survival rate, and grain production of the millet lines grown in the alkaline field (pH 9.10) of Ningxia Province, China, in 2021. Data are the means ± SEMs (*n* = 3 plots). (**E**) Statistical analysis of the survival rates of *Zm*WT and *ZmGS3*^{ko} grown in the alkaline field (pH 9.10) of Ningxia in 2021. Data are the means ± SEMs (*n* = 3 plots). In (A) to (E), statistical significance was determined by two-tailed

unpaired *t* test. *$P < 0.05$; **$P < 0.01$; ***$P < 0.001$; ****$P < 0.0001$. (**F**) A proposed model of the Gγ subunit AT1-mediated response to alkaline stress in plants. Under alkaline stress, PIP2s function as H_2O_2 exporters. The Gγ subunit AT1 could pair with Gβ to negatively modulate the phosphorylation level of PIP2s and thus reduce their H_2O_2 export activity, leading to overaccumulation of H_2O_2 and resulting in plant sensitivity to alkaline stress. The truncated form of AT1, at1, further inhibited H_2O_2 export activity and led to plant hypersensitivity to stress. However, the knockout of AT1 homologs or their natural nonfunctional form releases the inhibition of PIP2s and efficiently improves the alkaline stress tolerance of crops.

roles of water-facilitator type aquaporins in contributing to H_2O_2 detoxification to protect cells against oxidative stress.

With the knowledge that AT1 plays a negative role in modulating the phosphorylation of aquaporins to regulate the ROS level under alkaline stress conditions (Fig. 6F), we might be able to design crops that tolerate high alkaline stress. We have successfully demonstrated the potential alkaline tolerance improvement in a number of monocot crops (sorghum, rice, maize, and millet) by modifying *AT1* through knockout of *AT1* orthologs or selecting for nonfunctional alleles in *AT1* crops. This strategy might have potential value in other cereal crops. Other options to explore are the genetic engineering of *AT1* in dicotyledonous crops, such as tomatoes, potatoes, and fruit trees. The results may be even more complex because the *GS3* homolog has been reported to play opposite roles between dicots and monocots (*33*).

Materials and methods

Plant materials

Sixteen selected sorghum accessions based on seed availability belonging to a sorghum association panel (SAP) used in the study (*40*, *41*) were first used to screen the suitable concentration of alkaline treatment. The SAP population was composed of 352 sorghum inbred lines and was used to evaluate relative survival rates for GWASs. Seeds of the SAP population and another 37 sorghum accessions were all obtained from the United States Department of Agriculture's Agricultural Research Service (USDA-ARS). SN010 (of the Hap1 haplotype) is a sorghum variety from China, whereas M-81E (of Hap2) is a sorghum improved inbred from the United States. The NILs $AT1^{SN010}$ and $AT1^{M\text{-}81E}$ are from our laboratory stocks, and they differ in a 58-kb interval from that of the F_{11} generation. The interval was flanked by two molecular markers, *MSR0069* and *MSN0013*.

The rice NILs KY^{NIL}(*GS3*) and KY^{NIL}($gs3^{-}$) used in field trials were developed in the Kongyu131 (KY131) variety. Two rice varieties, Kongyu 131 (KY131) and Minghui 63 (MH63), were used as the parents for the construction of NILs. KY131, with a functional *GS3* allele, was used as the recipient and is a *japonica* variety with the largest planting area in China (https://www.ricedata.cn/variety/). MH63, with a nonfunctional *GS3-3* allele, was used as the donor and is an elite *indica*-type restorer line with the largest planting area in China. The overall construction followed a recurrent backcross procedure including four generations of backcrosses and two generations of selfing. A cross was made between the recipient KY131 and the donor MH63. In backcrossing generations from BC_1F_1 to BC_4F_1, selected individuals heterozygous at *GS3* were backcrossed to KY131. Negative selections were carried out in BC_3F_1, BC_4F_1, BC_4F_2, and BC_4F_3. In BC_3F_1 and BC_4F_1, the recombinants heterozygous at *GS3* were subjected to background selection using whole-genome array GSR40K. Subsequently, the BC_4F_3 population was developed from an individual in BC_4F_1 with the highest proportion of genome recovery of the sequence of the recurrent parent by two rounds of recombination selection. The genotype of an NIL from BC_4F_4 was further confirmed by whole-genome array GSR40K.

Zhongkefa5 (ZKF5) was generated from a cross between the recipient KY131 and Jiahe212 (containing a nonfunctional $gs3^{-}$ allele, a C to A mutation at position +16733441 of chromosome 3, and obtained a premature termination). Then, an F_1 individual was used as the recipient, and the landrace rice Songgen88 was used as the donor for subsequent backcrossing and selection. The *GS3-3* allele was confirmed by sequencing.

The sorghum transgenic overexpression line *SbAT1-OE* and mutant $SbAT1^{ko}$ used in this study were constructed in the sorghum variety Wheatland background. The millet $SiAT1^{I24}$ transgenic line and the $SiAT1^{ko}$ and $SiAT1^{I02}$ mutants used in this study were constructed in the millet variety Ci846 background. The rice *OsGS3-1OE*, *OsGS3-4OE*, $OsGS3^{ko}$, and *OsGS3Ri* transgenic lines with the ZH11 background have been previously described (*34*). The maize mutant line $ZmGS3^{ko}$ used in this study was developed using the maize variety KN5585. Related primers are shown in table S3.

Plant growth conditions

Before sowing, all seeds for each line that were plump and of similar size were chosen for study. Seeds were sterilized in 70% EtOH for 30 s and washed three times with distilled water. Subsequently, seeds were shaken in 10% bleach solution for 30 min and washed with distilled water 8 to 10 times. The seedlings were grown in a controlled greenhouse under long-day conditions (16 hours light/8 hours dark) at 28°C. The illumination was 600 μmol m^{-2} s^{-1}, and the relative humidity was 60 to 80%.

Field trials of sorghum, maize, and millet NILs and/or transgenic T_1 homozygous lines were carried out from April 2021 to September 2021 in Huiwei Village, Pingluo County of Ningxia Hui Autonomous Region (38°57′29″ N, 106°32′39″ E; elevation 1090 m). All the field tests in this study were performed with three plots as three repeats. The plot dimensions were 3.6 m by 1.5 m with row spacing of 0.5 m, plant spacing of 0.2 m, and walkways of 1 m between plots. Our sowing method was single-hole sowing, and the sowing depth was ~3 cm.

Field trials of rice KY NILs grown in sodic soil with a high pH of 9.17 were carried out in Honggangzi town, Jilin Province (45°36′19″ N, 123°50′55″ E; elevation 130 m). A pH 5.58 soil control was established by planting rice KY NILs in the same season in Heilongjiang (47°25′34″ N, 143°02′45″ E; elevation 80 m). One-month-old seedlings of each line cultivated in a greenhouse were selected and sown into the above paddy fields. The plot dimensions in the paddy fields were 1.5 m by 0.9 m, the row spacing was 0.3 m, and the plant spacing was 0.15 m. Three seedlings were transplanted per clump. Each plot had three replicates and was established based on a randomized block design. The field locations of ZKF5 plants grown in soils of pH 8.5 to 8.7 were 123°22′12″ to 124°54′ N and 45°23′24″ to 45°37′48″ E (composed of four plots, 7, 10, 8, and 8 ha separately), and those in soils of pH 7.4 to 7.6 were 122°48′36″ to 123°24′ N and 45°37′48″ to 45°39′36″ E (composed of two plots, 11 and 22 ha separately).

Phenotypic evaluation

The seeds used for phenotype evaluation were all harvested at the same time and stored under the same conditions. In an initial test, seeds of each of the 16 selected sorghum lines were sown uniformly in a nutrient soil with 50% vermiculite. Concentrations of 0, 25, 50, 75, 100, 125, and 150 mM mixed alkali ($NaHCO_3$:Na_2CO_3 with a molar ratio of 5:1) were used to immediately treat the soil. The 75 mM alkali treatment was selected as the most suitable concentration. The detailed working concentrations of $NaHCO_3$ and Na_2CO_3 in 75 mM alkali are 62.5 and 12.5 mM, respectively. It should be noted that the final concentration of mixed alkali is calculated based on the total volume of soil and absorbed water. Relative survival rate after plants spent 3 weeks under 75 mM alkali stress was recorded. The relative survival rate of a GWAS population was calculated by taking the numbers of survival plants under alkali stress and dividing it by the numbers of survival plants under standard conditions after 3 weeks of treatment. Thus,

the relative survival rate is contributed to by both the abilities of seed germination and seedling survival under alkali conditions. Three biological repeats for the phenotypic evaluation of the SAP population were performed. For transgenic and genome-edited plants, survival rates were recorded as the phenotypic data on the 14th day after the 75 mM mixed alkali stress treatment was applied. For phenotype evaluation of the field trials of sorghum, rice, maize, and millet plants, relative survival rates were calculated 1 month after sowing in the field, and other important agronomic traits, including biomass and grain yield, were recorded at maturity. The fresh weights of the aboveground materials of 10 seedlings from each line grown under the control and alkali treatments were also measured.

GWAS

Reference genome sequences of the sorghum variety BTx623 were obtained from a database of the Phytozome website (https://phytozome-next.jgi.doe.gov/) (*42*). SNP markers for the SAP population were obtained from the public community resource https://www.morrislab.org/data (*43*). SNPs with >20% missing data and minor allele frequencies (MAFs) below 0.05 were removed. A total of 82,430 SNPs for the SAP population were used for the GWAS and analyzed using a mixed linear model. The threshold for genome-wide significance was determined using Bonferroni correction, and significant differences were determined based on $P < 1 \times 10^{-5}$.

Bacterial strains and growth conditions

Escherichia coli strains XL1-Blue and DE3 were used for vector construction. XL1-Blue, separately transformed with each recombinant vector, was cultured in LB medium (1% tryptone, 0.5% yeast extract, and 1% NaCl) with an antibiotic (kanamycin or ampicillin) at 37°C overnight. *Agrobacterium tumefaciens* strains GV3101 and EHA105 harboring the corresponding recombinant vectors were liquid-cultured in the same LB medium with the appropriate antibiotics at 28°C overnight.

Plasmid construction and crop transformation

A *SbAT1* overexpression (*SbAT1-OE*) construct in sorghum was prepared by taking the full-length cDNAs of $SbAT1^{SN010}$ and cloning them into the pCambia2300-Myc vector with a Myc tag located at the N-terminal and driven by the ubiquitin promoter. A $SbAT1^{ko}$ mutant was constructed using a genome-editing system previously reported (*44*). A 20-bp–specific single-guide RNA (sgRNA) target sequence of Hap1 was synthesized and ligated to the pYLgRNA-*OsU6a* vector. The purified guide RNA (gRNA) expression cassette was subsequently inserted into the binary pYLCRISPR–Cas9-MB vector. *SbAT1-OE* and the recombinant pYLCRISPR–Cas9-MB plasmids were each introduced into the sorghum cultivar Wheatland (with the $SbAT1^{SN010}$ allele) through *Agrobacterium*-mediated transformation (performed in a crop transformation platform led by Y. Sui at the Biotechnology Research Institute, China Academy of Agriculture Sciences). The positive transgenic plants of the T_0 generation were identified by PCR. Gene expression levels of *SbAT1* in transgenic overexpression plants were detected by qPCR. Homozygous mutants of the T_1 generation were confirmed in the sgRNA target sequence by PCR.

We synthesized a truncated G protein γ subunit version of $SiAT1^{124}$, which mimicked the truncated $SbAT1^{M\text{-}81E}$. The $SiAT1^{124}$ overexpression construct was generated in the same pCambia2300-Myc vector as described above. The same genome-editing system (described above) was used to construct the $SiAT1^{ko}$ and $SiAT1^{102}$ mutants by designing the sgRNA target sequences in the second exon and the fifth exon of *SiAT1*, respectively. Each corresponding gRNA expression cassette was inserted into the final pYLCRISPR–Cas9-MH vector. All these successful constructs were introduced into the millet inbred line Ci846 (with the *SiAT1* allele) by *Agrobacterium*-mediated transformation. Positive transgenic overexpression plants of the T_0 generation were verified by PCR and qPCR. Homozygous mutants of the T_1 generation were identified in the designed sgRNA target sites by PCR.

The rice *OsGS3-1OE*, *OsGS3-4OE*, $OsGS3^{ko}$, and *OsGS3Ri* transgenic plants used in this study have been described in detail in previous studies (*34*).

A single mutant of $ZmGS3^{ko}$ (sgRNA designed in exon 1 and exon 2) with a 34-bp deletion was generated with the maize promoter *ZmU6* using the CRISPR-Cas9 system (*45*). The sgRNAs were designed using the website http://crispr.hzau.edu.cn/CRISPR2/. The vector confirmed by sequencing was introduced into *A. tumefaciens* EHA105 and transformed into the maize variety KN5585 by *Agrobacterium*-mediated transformation. Vector construction and plant transformation were performed by WIMI Biotechnology Co., Ltd. (China), as previously described (*45*). Mutations were confirmed by PCR sequencing samples from the T_0 and T_1 generations. All related primers are shown in table S3.

qPCR

Total RNA was extracted from fresh sorghum seedling roots by using a pure RNA extraction kit (Huayueyang, Beijing, China), with DNA digested by ribonuclease (RNase)–free Dnase I treatment. cDNA was obtained using a cDNA synthesis kit (TransGen, Beijing, China). qPCR was performed with the KOD SYBR qPCR Mix Kit (TransGen, Beijing, China) on an Applied Biosystems 7900HT Fast Real-Time PCR System. The relative expression of targeted genes was calculated by the relative quantification method ($2^{-\Delta\Delta CT}$). Three biological repeats were performed for each sample. The expression level of *SbEIF* was used to normalize all qPCR data. Related primers are shown in table S3.

Transient protein expression in Nicotiana benthamiana

Agrobacterium-mediated transient expression in *N. benthamiana* was performed according to a protocol described previously with some modifications (*46*). Approximately 1-month-old tobacco plants grown in a greenhouse under a 16-hours light/8-hours dark photoperiod were selected for infiltration. The *A. tumefaciens* strain EHA105 containing targeted gene vectors or the gene-silencing suppressor p19 was prepared. *Agrobacterium* colonies were inoculated into 5 ml of LB liquid medium with the appropriate antibiotics at 28°C and placed on a shaker overnight. Then, a 1/100 volume (50 μL) of the *Agrobacterium* culture was transferred into 5 ml of LB liquid medium with 40 μM acetosyringone (AS). After the OD_{600} (the optical density of a sample measured at a wavelength of 600 nm) reached ~3.0, bacteria were collected, and pellets were resuspended in 10 mM $MgCl_2$ to an OD_{600} of 1.5 for targeted genes and an OD_{600} of 1.0 for *p19*. Equal amounts of *Agrobacterium* transfected with targeted genes and *p19* were mixed. The mixed *Agrobacterium* solutions were kept still at room temperature for 2 to 5 hours and then infiltrated into the undersides of tobacco leaves. After 3 days, the leaf veins were removed, and the infiltrated tobacco leaves were collected for Western blot assays with the corresponding antibodies.

Protein expression in bacteria and purification

The plasmid for GST-AT1, GST-at1, or MBP-SbPIP2;1 protein expression was transformed into *E. coli* strain BL21 (DE3). A single colony was inoculated into 10 ml of liquid LB medium containing the ampicillin antibiotic and incubated at 37°C overnight. Then, the 10-ml culture was transferred into 300 ml of LB medium. When the OD_{600} reached 0.6 to 0.8, final concentrations of 0.8 mM isopropyl-β-D-thiogalactopyranoside (IPTG) and 0.2% glucose were added, and the bacteria were cultured at 18°C for 16 to 20 hours to induce fusion protein expression. The bacteria were lysed with a pressure machine (JNBIO), and glutathione Sepharose 4B beads (GE Healthcare) or amylase resin (NEB) was used for purification of the fusion proteins. The bound proteins were washed three times with 1× phosphate-buffered saline (PBS) buffer with 150 mM NaCl. MBP-PIP2;1 coated on the amylase resin was eluted by 10 mM maltose. The purified proteins GST-AT1 and GST-at1 coated on beads and eluted MBP-PIP2;1 were stored at −80°C until use.

LC-MS/MS assay

To obtain the interacting proteins of SbAT1, an LC-MS/MS assay was performed after a cell-free assay, which enriched the interacting proteins through incubation of the GST-SbAT1 protein with plant extracts. Seeds of the Wheatland sorghum were sown in soil supplemented with 75 mM alkali. Fourteen-day-old plants were collected and frozen in liquid nitrogen to be ground into fine powder. Native extraction buffer (50 mM Tris-MES at pH 8.0, 0.5 M sucrose, 1 mM $MgCl_2$, 10 mM EDTA, 5 mM DTT, 1 mM PMSF, Roche cOmplete Mini protease inhibitor cocktail tablets, and 0.2% NP40) was applied for total protein extraction. The plant extracts were centrifuged three times at 12,000 rpm for 10 min at 4°C, and the final protein supernatant was filtered with a 0.45-μm sterile membrane to remove the debris that could not be removed by centrifugation. GST-SbAT1 fusion proteins (200 ng) coated on beads were incubated with the above prepared plant protein extracts supplemented with MG132 (26S proteasome inhibitor) at 4°C for 3 hours, and then the beads were washed three times (for 10 min each time) with 1× PBS buffer along with 150 mM NaCl. The buffer was discarded completely after the last wash, and the beads were resuspended in 2× SDS protein loading buffer and heated at 95°C for 10 min. The sample was separated and purified by an SDS–polyacrylamide gel electrophoresis (SDS-PAGE) gel running for ~1 cm, and the gel was collected for in-gel digestion.

The gel sample containing GST-SbAT1 and its potential interacting proteins was cut into 2- to 3-mm^2 pieces in a dust-free environment. The destained gel pieces were treated with 10 mM DTT at 56°C for 1 hour and then with 55 mM iodoacetamide at room temperature in darkness for 45 min. Then, the proteins in the gel pieces were digested with trypsin (enzyme-to-substrate ratio 1:50) at 37°C overnight. The peptides were extracted from the gel pieces by sonication and freeze-dried in a SpeedVac concentrator. Finally, the peptides were redissolved in 0.1% formic acid and filtered through a 0.45-μm centrifugal filter before conducting the LC-MS/MS assay with a nanoLC-Q EXACTIVE mass spectrometer. The raw data were analyzed by Thermo Proteome Discoverer (1.4.0.288) and using the UniProt-proteome-*Sorghum bicolor* (*Sorghum vulgare*) database (strain: cv. BTx623) (20190715).

In the experiment identifying the phosphorylated sites in SbPIP2;1, the powder was lysed in a buffer containing 4% SDC and 100 mM Tris-HCl (pH 8.5). After sonication, the lysates were centrifuged for 10 min at 12,000 g to remove insoluble debris. Protein (~1200 μg) was reduced and alkylated by TCEP and CAA and digested with trypsin (1:50 w/w) at 37°C overnight. After digestion, the phosphopeptides were enriched using titanium dioxide beads (TiO_2; GL Sciences, 5010-21315). The phosphopeptides were analyzed by an Orbitrap Fusion Lumos Tribrid mass spectrometer (Thermo Scientific, Rockford, IL Waltham, MA) coupled online to an Easy-nLC 1000 in the data-dependent mode. Precursor ions were measured in the Orbitrap analyser at 240,000 resolution. The twenty most intense ions from each MS scan were isolated and fragmented by high-energy collisional dissociation. The database search was performed for all raw MS files using the software MaxQuant (version 1.6.3.4). The *S. bicolor* proteome sequence database was applied to search the data. Serine, threonine, and tyrosine phosphorylation; protein N-terminal acetylation; and methionine oxidation were included in the search as the variable modifications. Cysteine carbamidomethylation was set as a stable modification.

LCI assay

LCI assays were carried out following a method published previously (*29*). The coding sequences of targeted genes or a control gene were cloned into pCAMBIA1300-nLUC or pCAMBIA1300-cLUC, respectively. The constructs Nluc-SbAT1, Nluc-Sbat1, Nluc-OsGS3-1, Nluc-OsGS3-4, Cluc-SbPIP2;1, Cluc-OsPIP2;1, and Cluc-SbTGA1 were then transformed into *A. tumefaciens* strain GV3101. As described in the section on protein transient expression in tobacco leaves, equal amounts of bacteria harboring different constructs and *p19* were mixed and infiltrated into tobacco leaves. After 3 days, 1 mM luciferin substrate was spread evenly on the underside of leaves and allowed to react for 5 min in the dark. Subsequently, luciferase activity signals were detected with a cooled low-light charge-coupled device camera (Night OWL II LB 983).

Pull-down assay

To investigate the direct interaction of SbAT1 or Sbat1 with SbPIP2;1, the GST-SbAT1, GST-Sbat1, and MBP-SbPIP2;1 fusions were expressed in *E. coli* strain BL21 (DE3) and purified with glutathione Sepharose 4B beads or amylase resin (NEB), as described above. Equimolar amounts of GST, GST-SbAT1, and GST-Sbat1 proteins coated on beads were incubated with equal amounts of eluted MBP-SbPIP2;1 protein at 4°C for 2 hours. Then, the beads were washed five times with 1× PBS containing 150 mM NaCl. All the supernatant was removed and transferred into 2× SDS protein loading buffer before heating at 95°C for 10 min. The eluted proteins were examined by Western blot with an anti-MBP antibody.

Co-IP assay

GFP, GFP-SbAT1, GFP-Sbat1, and Cluc-SbPIP2;1 proteins were transiently expressed in tobacco leaves. The samples were ground into powder in liquid nitrogen, and the protein extracts were prepared with native extraction buffer supplemented with MG132. GFP, GFP-SbAT1, and GFP-Sbat1 protein extracts were enriched with magnetic beads coated with an anti-GFP antibody and then placed at 4°C for 2 hours. The beads were then washed three times with 1× PBS buffer. Equal amounts of Cluc-SbPIP2;1 protein extracts were added to the beads and incubated at 4°C for 2 hours. After washing three times with 1× PBS supplemented with 150 mM NaCl, the bead samples were placed into 2× SDS protein loading buffer and heated at 95°C for 10 min. Finally, the precipitates were analyzed by Western blotting with an anti-Luc antibody.

Detection of redox states in protoplasts by confocal microscopy and microplate reader

Redox states assays determined by Cyto-roGFP2-Orp1 were performed as described by Gutscher *et al.* (*29*). Briefly, genes encoding Cyto-roGFP2-Orp1 were cloned into the pGFP2 vector and to generate pGFP2-Cyto-roGFP2-Orp1. Protoplasts were prepared with 10-day-old rice seedlings grown in a sterile container. Protoplasts overexpressed the Cyto-roGFP2-Orp1 probe by the PEG transfection method. After 12 to 16 hours, the protoplasts were centrifuged gently at 100 g for 3 min, the supernatant was removed and the protoplasts were resuspended in W5 liquid buffer (154 mM NaCl, 125 mM $CaCl_2$, 5 mM KCl, 2 mM MES) with different pH for 40 min. Then the redox states of those rice protoplasts were analyzed by confocal microscopy and microplate reader. A total of 1×10^5 sample protoplasts were used for microplate reader analyzing in each sample repeat. For mircroscopy assay, transfected protoplasts were set on glass bottom dishes and analyzed using a laser scanning confocal microscopy system (LSM 710, Carl Zeiss) with a Plan-Apochromat 63× oil immersion lens (NA 1.4), and then the redox states of those rice protoplasts were analyzed using a laser scanning confocal microscopy system (LSM 710, Carl Zeiss). Fluorescence ratiometric intensity images (1024 × 1024 points, 16 bits) of protoplasts were acquired. A 405-nm diode and 488-nm argon lasers (or 458-nm diode) were used for excitation. The signal was detected with 510- to 550-nm filters. Images were analyzed using ImageJ (National Institutes of Health) and Zen (Carl Zeiss) softwares, and the ratio of 405/488 nm indicated the relative level of H_2O_2.

The redox states of protoplasts overexpressing Cyto-roGFP2-Orp1 were detected using a microplate reader (Thermo Scientific Varioskan LUX). We measured Cyto-roGFP2-Orp1 at 525 nm after excitation at 405 and 488 nm in a black plate reader. The background of the fluorescence value produced by untransfected protoplasts was subtracted, and the ratio of 405/488 nm indicated the relative level of H_2O_2. All the raw and non-normalized data were shown in table S4.

ROS, H_2O_2, and relative chlorophyll content detection

The formation of peroxides in the leaves was investigated by the 3,3′-diaminobenzidine (DAB) staining method (*47*). Seedling leaves of the control (CK) and alkali treatments were soaked in 10 ml of staining buffer (50 mM Na_2HPO_4 and DAB). After vacuuming, the samples were incubated overnight in the dark at room temperature. Samples were transferred to an eluent (anhydrous ethanol:glacial acetic acid:glycerol = 3:1:1) and boiled for 10 min to remove chlorophyll, and then the images of samples were taken under the same condition.

For the detection of cytosolic ROS levels in the root tips of *PIP2;1* and Gγ subunit-related genetic plants, the dye OxyBURST Green H_2DCFDA (Molecular Probes D-2935, Thermo Fisher Scientific) was used with staining method described before (*48*). Two-week-old sorghum and rice seedlings grown in soil culture under normal conditions treated with or without 200 mM alkali for 48 hours were used for analysis. Then, the lateral roots of the alkali-treated and control-treated seedlings were collected, cleanly rinsed, and gently transferred to 50-ml tubes. H_2DCFDA was primarily dissolved in dimethyl sulfoxide (DMSO) to 10 mM and then diluted with sample buffer (10 mM Tris-HCl, 50 mM KCl, pH 7.2) into a final concentration of 50 μM for use. Samples were soaked in 0.01% Tween 20 and vacuumed for 30 min, rinsed twice with distilled water, and then washed with washing buffer (10 mM Tris-HCl pH 7.2 and 50 mM KCl). Samples were subsequently incubated with 50 μM H_2DCFDA staining solution in the dark at room temperature for 10 min, and the excess dye was removed with distilled water twice. For the detection of apolast ROS accumulation, samples were prepared as the detection of cytosolic ROS above. Each sample was soaked with OxyBURST Green H_2HFF BSA (100 μg ml^{-1}) dissolved in 1× PBS buffer for 45 min in the dark, and then washed with distilled water to remove the excess dye. All the samples were examined using a Zeiss LSM 510 confocal microscope with 488-nm excitation and 530-nm emission. To compare the fluorescence intensity, all axes of parameters from different experimental conditions were fixed simultaneously and analyzed under the confocal microscope by using the same settings.

Five to 20 lateral roots of each sample were chosen, and one to three visual fields of each lateral root were selected for imaging. For quantification of the intracellular ROS accumulation at the single–root cell level, three representative root cells of each visual field were selected for statistical data. The average value of fluorescence intensity was recorded as one replicate. For quantification of extracellular ROS accumulation at the single–root cell level, one representative single cell was selected for each visual field. A typical root cell contains a rectangular contour, including two lengths and two widths. The sum of rectangular contour was recorded as the fluorescence intensity of each replicate. The final average value of all repetitions was taken as the fluorescence intensity of each sample.

A portable SPAD-502 handheld chlorophyll meter (Minolta, Osaka, Japan) was used to noninvasively measure the relative chlorophyll content of seedling leaves. Six biological repeats were performed.

Quantification and statistical analyses

For image quantification of H_2O_2 detection, six unsaturated confocal images were selected and analyzed with ImageJ software (https://imagej.nih.gov/ij/). All data plotting and statistical analyses were performed with GraphPad Prism 8.0 software (https://www.graphpad.com/). Details about the statistical parameters, such as the means ± SDs (standard deviations), SEs (standard errors), and 95% confidence intervals, are shown in the figure legends. A two-tailed Student's *t* test for two groups or a one-way analysis of variance (ANOVA) with Dunnett's or Tukey's multiple comparisons test for multiple groups were carried out. The number of samples is represented by *n*. Asterisks indicate statistical significance: $^*P < 0.05$; $^{**}P < 0.01$; $^{***}P < 0.001$; $^{****}P < 0.0001$; NS, not significant.

REFERENCES AND NOTES

1. A. Kumar, S. Singh, A. K. Gaurav, S. Srivastava, J. P. Verma, Plant growth-promoting bacteria: Biological tools for the mitigation of salinity stress in plants. *Front. Microbiol.* **11**, 1216 (2020). doi: 10.3389/fmicb.2020.01216; pmid: 32733391
2. B. P. Singh, A. L. Cowie, K. Y. Chan, Eds., *Soil Health and Climate Change*, vol. 29 of *Soil Biology* (Springer, 2011).
3. M. Javid, R. Ford, M. E. Nicolas, Tolerance responses of *Brassica juncea* to salinity, alkalinity and alkaline salinity. *Funct. Plant Biol.* **39**, 699–707 (2012). doi: 10.1071/FP12109; pmid: 32480821
4. G. K. S. Ananda *et al*., Wild sorghum as a promising resource for crop improvement. *Front. Plant Sci.* **11**, 1108 (2020). doi: 10.3389/fpls.2020.01108; pmid: 32765575
5. X. Sun *et al*., A *Glycine soja* methionine sulfoxide reductase B5a interacts with the Ca^{2+}/CAM-binding kinase GsCBRLK and activates ROS signaling under carbonate alkaline stress. *Plant J.* **86**, 514–529 (2016). doi: 10.1111/tpj.13187; pmid: 27121031
6. H. Zhang *et al*., Root damage under alkaline stress is associated with reactive oxygen species accumulation in rice (*Oryza sativa* L.). *Front. Plant Sci.* **8**, 1580 (2017). doi: 10.3389/fpls.2017.01580; pmid: 28943882
7. M. An *et al*., Application of compound material alleviates saline and alkaline stress in cotton leaves through regulation of the transcriptome. *BMC Plant Biol.* **20**, 462 (2020). doi: 10.1186/s12870-020-02649-0; pmid: 33032521
8. G. P. Bienert, F. Chaumont, Aquaporin-facilitated transmembrane diffusion of hydrogen peroxide. *Biochim. Biophys. Acta* **1840**, 1596–1604 (2014). doi: 10.1016/j.bbagen.2013.09.017; pmid: 24060746
9. H. Tong *et al*., A *Streptococcus* aquaporin acts as peroxiporin for efflux of cellular hydrogen peroxide and alleviation of oxidative stress. *J. Biol. Chem.* **294**, 4583–4595 (2019). doi: 10.1074/jbc.RA118.006877; pmid: 30705089
10. K. Varadaraj, S. S. Kumari, Lens aquaporins function as peroxiporins to facilitate membrane transport of hydrogen peroxide. *Biochem. Biophys. Res. Commun.* **524**, 1025–1029 (2020). doi: 10.1016/j.bbrc.2020.02.031; pmid: 32063362
11. Q. Chen *et al*., ERAD-related E2 and E3 enzymes modulate the drought response by regulating the stability of PIP2 aquaporins. *Plant Cell* **33**, 2883–2898 (2021). doi: 10.1093/plcell/koab141; pmid: 34015125
12. O. Rodrigues *et al*., Aquaporins facilitate hydrogen peroxide entry into guard cells to mediate ABA- and pathogen-triggered stomatal closure. *Proc. Natl. Acad. Sci. U.S.A.* **114**, 9200–9205 (2017). doi: 10.1073/pnas.1704754114; pmid: 28784763
13. S. Pandey, Heterotrimeric G-protein signaling in plants: Conserved and novel mechanisms. *Annu. Rev. Plant Biol.* **70**, 213–238 (2019). doi: 10.1146/annurev-arplant-050718-100231; pmid: 31035831
14. M. N. Haque *et al*., Characteristics of arsenic adsorption to sorghum biomass. *J. Hazard. Mater.* **145**, 30–35 (2007). doi: 10.1016/j.jhazmat.2006.10.080; pmid: 17241742
15. S. Griebel, A. Adedayo, M. R. Tuinstra, Genetic diversity for starch quality and alkali spreading value in sorghum. *Plant Genome* **14**, e20067 (2021). doi: 10.1002/tpg2.20067; pmid: 33259143
16. H. Mao *et al*., Linking differential domain functions of the GS3 protein to natural variation of grain size in rice. *Proc. Natl. Acad. Sci. U.S.A.* **107**, 19579–19584 (2010). doi: 10.1073/pnas.1014419107; pmid: 20974950
17. Q. Li *et al*., Cloning and characterization of a putative *GS3* ortholog involved in maize kernel development. *Theor. Appl. Genet.* **120**, 753–763 (2010). doi: 10.1007/s00122-009-1196-x; pmid: 19898828
18. P. Xie *et al*., Natural variation in *Glume Coverage 1* causes naked grains in sorghum. *Nat. Commun.* **13**, 1068 (2022). doi: 10.1038/s41467-022-28680-3; pmid: 35217660
19. C. Fan *et al*., *GS3*, a major QTL for grain length and weight and minor QTL for grain width and thickness in rice, encodes a putative transmembrane protein. *Theor. Appl. Genet.* **112**, 1164–1171 (2006). doi: 10.1007/s00122-006-0218-1; pmid: 16453132
20. S. M. Assmann, Heterotrimeric and unconventional GTP binding proteins in plant cell signaling. *Plant Cell* **14**, S355–S373 (2002). doi: 10.1105/tpc.001792; pmid: 12045288
21. B. R. Temple, A. M. Jones, The plant heterotrimeric G-protein complex. *Annu. Rev. Plant Biol.* **58**, 249–266 (2007). doi: 10.1146/annurev.arplant.58.032806.103827; pmid: 17201690
22. Y. Trusov, D. Chakravorty, J. R. Botella, Diversity of heterotrimeric G-protein γ subunits in plants. *BMC Res. Notes* **5**, 608 (2012). doi: 10.1186/1756-0500-5-608; pmid: 23113884
23. N. Smirnoff, D. Arnaud, Hydrogen peroxide metabolism and functions in plants. *New Phytol.* **221**, 1197–1214 (2019). doi: 10.1111/nph.15488; pmid: 30222198
24. S. Tian *et al*., Plant aquaporin AtPIP1;4 links apoplastic H_2O_2 induction to disease immunity pathways. *Plant Physiol.* **171**, 1635–1650 (2016). doi: 10.1104/pp.15.01237; pmid: 26945050
25. M. Oparka *et al*., Quantifying ROS levels using CM-H_2DCFDA and HyPer. *Methods* **109**, 3–11 (2016). doi: 10.1016/j.ymeth.2016.06.008; pmid: 27302663
26. B. Morgan, M. C. Sobotta, T. P. Dick, Measuring E_{GSH} and H_2O_2 with roGFP2-based redox probes. *Free Radic. Biol. Med.* **51**, 1943–1951 (2011). doi: 10.1016/j.freeradbiomed.2011.08.035; pmid: 21964034
27. A. V. Baranova, Y. L. Orlov, The papers presented at 7th Young Scientists School "Systems biology and bioinformatics" (SBB'15): Introductory note. *BMC Genet.* **17**, S20 (2016). doi: 10.1186/s12863-015-0326-5; pmid: 26822407
28. R. E. Carmichael, A. Boyce, C. Matthewman, N. J. Patron, An introduction to synthetic biology in plant systems. *New Phytol.* **208**, 20–22 (2015). doi: 10.1111/nph.13433; pmid: 26311282
29. M. Gutscher *et al*., Proximity-based protein thiol oxidation by H_2O_2-scavenging peroxidases. *J. Biol. Chem.* **284**, 31532–31540 (2009). doi: 10.1074/jbc.M109.059246; pmid: 19755417
30. C. J. Huang, X. H. Wang, J. Y. Huang, C. G. Zhang, Y. L. Chen, Phosphorylation of plasma membrane aquaporin PIP2;1 in C-terminal affects light-induced stomatal opening in *Arabidopsis*. *Plant Signal. Behav.* **15**, 1795394 (2020). doi: 10.1080/15592324.2020.1795394; pmid: 32693667
31. D. Qing *et al*., Quantitative and functional phosphoproteomic analysis reveals that ethylene regulates water transport via the C-terminal phosphorylation of aquaporin PIP2;1 in Arabidopsis. *Mol. Plant* **9**, 158–174 (2016). doi: 10.1016/j.molp.2015.10.001; pmid: 26476206
32. A. L. Szymczak *et al*., Correction of multi-gene deficiency *in vivo* using a single 'self-cleaving' 2A peptide–based retroviral

vector. *Nat. Biotechnol.* **22**, 589–594 (2004). doi: 10.1038/nbt957; pmid: 15064769
33. S. Sun *et al*., A G-protein pathway determines grain size in rice. *Nat. Commun.* **9**, 851 (2018). doi: 10.1038/s41467-018-03141-y; pmid: 29487318
34. W. Yang *et al*., The RING E3 ligase CLG1 targets GS3 for degradation via the endosome pathway to determine grain size in rice. *Mol. Plant* **14**, 1699–1713 (2021). doi: 10.1016/j.molp.2021.06.027; pmid: 34216830
35. Y. Tao *et al*., Large-scale GWAS in sorghum reveals common genetic control of grain size among cereals. *Plant Biotechnol. J.* **18**, 1093–1105 (2020). doi: 10.1111/pbi.13284 pmid: 31659829
36. Y. Cui, N. Jiang, Z. Xu, Q. Xu, Heterotrimeric G protein are involved in the regulation of multiple agronomic traits and stress tolerance in rice. *BMC Plant Biol.* **20**, 90 (2020). doi: 10.1186/s12870-020-2289-6; pmid: 32111163
37. G. Zou *et al*., Sorghum *qTGW1a* encodes a G-protein subunit and acts as a negative regulator of grain size. *J. Exp. Bot.* **71**, 5389–5401 (2020). doi: 10.1093/jxb/eraa277; pmid: 32497208
38. N. Takano-Kai, K. Doi, A. Yoshimura, *GS3* participates in stigma exsertion as well as seed length in rice. *Breed. Sci.* **61**, 244–250 (2011). doi: 10.1270/jsbbs.61.244
39. Y. Kan *et al*., *TT2* controls rice thermotolerance through SCT1-dependent alteration of wax biosynthesis. *Nat. Plants* **8**, 53–67 (2022). doi: 10.1038/s41477-021-01039-0; pmid: 34992240
40. G. P. Morris *et al*., Population genomic and genome-wide association studies of agroclimatic traits in sorghum. *Proc. Natl. Acad. Sci. U.S.A.* **110**, 453–458 (2013). doi: 10.1073/pnas.1215985110; pmid: 23267105
41. D. M. Goodstein *et al*., Phytozome: A comparative platform for green plant genomics. *Nucleic Acids Res.* **40**, D1178–D1186 (2012). doi: 10.1093/nar/gkr944; pmid: 22110026
42. M. Li, N. Yuyama, L. Luo, M. Hirata, H. Cai, In silico mapping of 1758 new SSR markers developed from public genomic sequences for sorghum. *Mol. Breed.* **24**, 41–47 (2009). doi: 10.1007/s11032-009-9270-2
43. X. Ma *et al*., A robust CRISPR/Cas9 system for convenient, high-efficiency multiplex genome editing in monocot and dicot plants. *Mol. Plant* **8**, 1274–1284 (2015). doi: 10.1016/j.molp.2015.04.007; pmid: 25917172
44. H. J. Liu *et al*., High-throughput CRISPR/Cas9 mutagenesis streamlines trait gene identification in Maize. *Plant Cell* **32**, 1397–1413 (2020). doi: 10.1105/tpc.19.00934; pmid: 32102844
45. L. Liu *et al*., An efficient system to detect protein ubiquitination by agroinfiltration in *Nicotiana benthamiana*. *Plant J.* **61**, 893–903 (2010). doi: 10.1111/j.1365-313X.2009.04109.x; pmid: 20015064
46. H. Chen *et al*., Firefly luciferase complementation imaging assay for protein-protein interactions in plants. *Plant Physiol.* **146**, 323–324 (2008). doi: 10.1104/pp.107.111740; pmid: 18065554
47. N. Jambunathan, in *Plant Stress Tolerance*, R. Sunkar, Ed., vol. 639 of *Methods in Molecular Biology* (Humana Press, 2010), pp. 291–297.
48. G. B. Monshausen, T. N. Bibikova, M. A. Messerli, C. Shi, S. Gilroy, Oscillations in extracellular pH and reactive oxygen species modulate tip growth of *Arabidopsis* root hairs. *Proc. Natl. Acad. Sci. U.S.A.* **104**, 20996–21001 (2007). doi: 10.1073/pnas.0708586104; pmid: 18079291

ACKNOWLEDGMENTS

We thank the US Department of Agriculture–Agricultural Research Service (USDA-ARS) for providing sorghum seeds for the sorghum association panel. We are grateful to N. Li from the Hong Kong University of Science and Technology for providing the anti-PIP2.1 (pS285/288) antibody and to C. Chu from Huanan Agriculture University for providing the genome sequence of the rice lines. **Funding:** This work was supported by National Natural Science Foundation of China grants U1906204 (to Q.X.) and 32222010 (to F.Y.), Strategic Priority Research Program of the Chinese Academy of Sciences grant XDA24010306 (to Q.X.), Agricultural Breeding Program in NingXia Province grant 2019NYYZ04 (to Q.X. and X.Xu), National Natural Science Foundation of China grant 31821005 (to Q.Z.), and Chinese Universities Scientific Fund grant 1201–15052001 (to F.Y.). S.T. is supported by the Youth Innovation Promotion Association of the Chinese Academy of Sciences. **Author contributions:** Q.X. conceived the project. Q.X., F.Y., and Y.O. designed the research procedure. H.Z., F.Y., P.X., S.S., X.Q., S.T., C.M., D.Y., X.H., and Z.F. performed the experiments. Che.C., H.Y., J.Lu, Q.Z., Y.Wu, R.X., Y.Wa., and Cha.C. analyzed the data. S.Y., X.L., J.Li, Y.L., X.Xi., D.M., X.Xu, Z.L., G.L., J.Lu, and Q.Z. provided field tests and guidance. Q.X. and F.Y. wrote the manuscript with input from all authors. **Competing interests:** Patent applications related to this work have been submitted by Q.X., F.Y., H.Z., Y.O., and Q.Z. All other authors declare no competing interests. **Data and materials availability:** All data needed to evaluate the conclusions in the paper are present in the paper or the supplementary materials. Rice- and maize-related materials are available from Y.O. and sorghum- and millet-related materials are available from Q.X. under a material transfer agreement with the Institute of Genetics and Developmental Biology or Huazhong Agricultural University, respectively.

SUPPLEMENTARY MATERIALS

science.org/doi/10.1126/science.ade8416
Figs. S1 to S7
Tables S1 to S4
MDAR Reproducibility Checklist

View/request a protocol for this paper from *Bio-protocol*.

Submitted 16 September 2022; accepted 8 February 2023
10.1126/science.ade8416